Ceramics International

Optimisation on the stability of CaO-doped partially stabilised zirconia by microwave heating

--Manuscript Draft--

Manuscript Number:	CERI-D-20-10499R2
Article Type:	Full length article
Keywords:	microwave heating; calcium oxide doped partially stabilised zirconia; stability ratio; phase transition
Corresponding Author:	Lei Gao, Ph.D Yunnan Minzu University Kunming, CHINA
First Author:	Yeqing Ling
Order of Authors:	Yeqing Ling
	Qiannan Li
	Hewen Zheng
	Mamdouh Omran
	Lei Gao, Ph.D
	Jin Chen
	Guo Chen
Abstract:	Partially stabilised zirconia has advantages for the applications in the metallurgical processes which have special requirements in corrosion resistance and high-temperature performance. In the present work, controllable microwave heating was used for the uniform thermal field and consequent microstructure improvement to further improve the stability of partially stabilised zirconia, which was 88.14% prepared by electric arc melting. Analyses including X-ray diffraction (XRD), Scanning electron microscopy (SEM), Fourier transform infrared spectroscopy (FTIR) and Raman spectroscopy (Raman) were used to study the effect of temperature change on the phase composition and structure of the samples. After heating at temperatures of 900 °C, 1000 °C, 1100 °C, 1200 °C and 1300 °C for 1h, the stabilities of the heated product were 88.51%, 95.02%, 95.17%, 96.31% and 97.64%, respectively. From the phase transformations based on the experimental results, the discussion indicates that the martensitic transformation temperature of zirconia from m-ZrO 2 to t-ZrO 2 during the heating stage was reduced under the radiation of microwave energy.

Optimisation on the stability of CaO-doped partially stabilised zirconia by microwave heating

Yeqing Ling [a, b], Qiannan Li [a, b], Hewen Zheng [a, b], Mamdouh Omran [c], Lei Gao [a, *], Jin Chen [b, **], Guo Chen [a, b, **]

[a] *Kunming Key Laboratory of Energy Materials Chemistry, Key Laboratory of Green-Chemistry Materials in University of Yunnan Province, Yunnan Minzu University, Kunming 650500, PR China.*

[b] *Key Laboratory of Unconventional Metallurgy, Ministry of Education, Kunming University of Science and Technology, Kunming 650500, PR China.*

[c] *Faculty of Technology, University of Oulu, Finland.*

[*] Corresponding author: glkust2013@hotmail.com

[**] Co-corresponding author: jinchen@kust.edu.cn, guochen@kust.edu.cn

Abstract

Partially stabilised zirconia has advantages for the applications in the metallurgical processes which have special requirements in corrosion resistance and high-temperature performance. In the present work, controllable microwave heating was used for the uniform thermal field and consequent microstructure improvement to further improve the stability of partially stabilised zirconia, which was 88.14% prepared by electric arc melting. Analyses including X-ray diffraction (XRD), Scanning electron microscopy (SEM), Fourier transform infrared spectroscopy (FTIR) and Raman spectroscopy (Raman) were used to study the effect of temperature change on the phase composition and structure of the samples. After heating at temperatures of 900 °C, 1000 °C, 1100 °C, 1200 °C and 1300 °C for 1h, the stabilities of the

heated product were 88.51%, 95.02%, 95.17%, 96.31% and 97.64%, respectively. From the phase transformations based on the experimental results, the discussion indicates that the martensitic transformation temperature of zirconia from m-ZrO_2 to t-ZrO_2 during the heating stage was reduced under the radiation of microwave energy.

Keywords: microwave heating

; calcium oxide doped partially stabilised zirconia; stability ratio; phase transition

1 Introduction

Zirconia (ZrO_2) has excellent properties for industrial applications, which have the advantages of high melting point and hardness, low thermal conductivity and thermal expansion coefficient, high refractive index and dielectric parameters, good biocompatibility, difficult corrosion. Therefore, zirconia has become an important inorganic nonmetallic material and has been widely concerned for the applications including refractory, gas turbine, ceramic materials and grinding materials. However, pure zirconia performs unsatisfactory thermal-shock resistance during high-temperature heating or cooling treatment process, resulting from volume-expansion-induced cracking. The cracking occurs because of phase transformation and the subsequent changes in shear stress and volume[1]. For the phase transformation of tetragonal(t-ZrO_2)-to-monoclinic (m-ZrO_2), crackings appear in a normal transformation direction at a temperature below 1000 °C, and also happens in a reverse transformation direction above the temperature of 1173 °C[2-4].

To improve the stability of various properties of ZrO_2, one promising solution is to dope stabilisers to replace Zr^{4+} ion and consequently forming a stable replacement solid solution, which will optimise the internal microstructure of the crystal structure[5]. Various studies have

shown that suitable doping stabilisers including Y_2O_3[6], CaO[7], Al_2O_3, MgO[8] and Sc_2O_3. As a result of doping, the cell volume in zirconia increases, thus the vacancy around zirconium ion reduces the repulsive force between O^{2-}-O^{2-} in the crystal, leading to a distorted coordination layer which effectively inhibits the phase transformation. Consequently, doping prevents the martensitic phase transformation, and thus keeps the tetragonal phase with during the cooling process [9-11]. By controlling the quantity and type of stabilisers, ZrO_2 can be divided into three types of materials from the perspective of microstructure with different stable states doped and crystal size. The mentioned types of ZrO_2 are tetragonal zirconia polycrystalline (TZP), fully stabilised zirconia (FSZ) and partially stabilised zirconia (PSZ) which is a vigorous developed toughening ceramic material contains the tetragonal phase of zirconia[12]. At present, the main preparation method of PSZ ceramic materials is the arc melting method which has high requirements on temperature and disadvantages including long operation time and large energy consumption. The technique also results in low performance on the stability of prepared PSZ materials, which greatly limits the application of this potential ceramic material[13]. It is urgent to develop a low consumption and high-performance preparation method for PSZ ceramic.

Microwave heating technology has great potential as an alternative method for the preparation of PSZ ceramic and has received wide attention[14, 15]. The concept of microwave heating technology was firstly proposed in the mid-1960s[16]. In the middle and late 1980s, microwave heating technology was introduced into the fast preparation of materials and was used as an alternative heating method for the preparation of powder metal[17]. After the 1990s, the technology has developed rapidly in the fields of mineral processing, polymer, nano-organic synthesis and the preparation of special materials. Nowadays, microwave heating

technology has become a key technical method for the efficient preparation of various optimised and modified novel materials based on its advantages[18-20], including selective heating, effective refinement on particle size and microstructure and improved heating uniformity[21-23]. These advantages are resulting from the unique microwave heating mechanism. Microwave can penetrate materials since it is a kind of high-frequency electromagnetic wave(0.3Hz-300GHz). Under the radiation of microwave energy, the material can be fast heated with a uniform thermal field resulting from dielectric loss determined by the microwave absorbing properties including dielectric constant and loss tangent coefficient. A series of studies on the preparation and treatment of ores by the microwave-assisted method were carried out, and FeMn78C8.0 bulk with high density property and low phosphorus was successfully prepared by green microwave heating process[19]; Microwave carbon thermal reduction process for the treatment of manganese ore was used and provided an application reference for microwave reduction of biomass minerals[24, 25]; The microwave drying characteristics of manganese ore were investigated along with the drying mechanism using dynamics and fitting analysis, thus microwave absorption rate in high water content area was promoted [26]. Monaco et al. [27] studied the possibility of low-temperature preparation of ZrO_2 by single-mode and multi-mode microwave heating methods, respectively. At the heating temperature of 1200 °C and the heating cycle of 6 min, the same density can be achieved as that of traditional heating (1450 °C, 600 min). Yan et al. [28] studied the effects of heating temperature and holding time on the mechanical properties of ultrafine Ti (C, N) - based cermets. The results show that the shrinkage, density, bending strength and hardness of ultrafine Ti (C, N) - based cermets increase with the heating temperature increasing to 1500 °C. The results show that the material has fine grains and excellent properties at 1500 °C

for 30 min. Ahmad et al. [29] prepared polycrystalline yttrium aluminium garnet (YAG) ceramic by microwave heating. Micron-sized of Al_2O_3 and Y_2O_3 powders were mixed through in house fabrication mixer for 24 hours before calcined at 1100 °C and palletization process. While both grain sizes and density of heated samples were found increased from 1.4 μm to 2.46 μm and 90% to 98%, respectively. Therefore, microwave heating has a significant effect on the densification behaviour of YAG.

Under the action of the microwave electromagnetic field, ceramic materials will produce a series of dielectric polarization, such as electronic polarization, atomic polarization, dipole turn polarization and interface polarization. In the previous study, $Ba_{0.5}Sr_{0.5}Co_{0.8}Fe_{0.2}O_{3-\delta}$ (BSCF) cathode layer for fuel cells was prepared by a method based on microwave heating[30]. Different from the traditional preparation method for BSCF with a heating temperature of 1000 °C for several hours, the cathode layer can be well bonded with BSCF after heating at 900 °C for 10 minutes under microwave condition. The BSCF layer maintains the microstructure required for the cathodic reaction, effectively reduces the element diffusion between the cathode layer and $BaZr_{0.1}Ce_{0.7}Y_{0.2}O_{3-\delta}$ electrolyte and improves the resistance value. Besides, the power output of BSCF-battery in the microwave group is 0.96 W/cm^2 at 700 °C, which is higher than that of conventional cathode-battery (0.33 W/cm^2). Al_2O_3 ceramics and Al_2O_3 matrix composites with different graphene nanoplatelets (GPL) content were prepared by microwave heating at 1500 °C[31]. The dispersion of GPL in N-methyl pyrrolidone was optimised to depolymerise GPL without destroying its structure. With the addition of GPLs, the microstructure of the composites was further refined and the compactness of the composites was improved. With an optimised value of GPLs% equals to 0.4%, the hardness, fracture toughness and bending strength of the prepared specimen are in

the best state. The research shows that compared with that prepared by conventional heating, ceramic materials prepared by microwave heating have higher density and hardness, more uniform microstructure and better toughness, and the technology was also noticed with high operation efficiency and low energy consumption[32, 33]. Christophe et al. [34] investigated a better understanding of the effect of multimode-microwave heating of zirconia-toughened alumina (ZTA). A comparative dilatometric analysis was conducted between conventional and microwave heating processes, to clarify the influence of zirconia on the densification of ZTA under electromagnetic field. Microwave heating creates a finer homogeneous microstructure, with resulting hardness and toughening comparable to those obtained for conventional heating[35]. Compared with conventional methods, the microwave hybrid heating on ZTA reaches almost full density in a shorter time cycle and at a lower heating temperature. Furthermore, microwave heating is a good way to suppress the grain growth of ZTA and to provide a more uniform microstructure. Furthermore, Benavente et al. [36] have shown that ZTA composites heated by microwave have higher density, hardness and young's modulus in comparison to conventional heating. Therefore, replacing conventional heating with microwave heating could effectively enhance the product yield of PSZ ceramic with the advantages including strong penetration, non-ionization and green energy-saving. In our previous study, the influence of microwave heating time on the stability performance was introduced[37, 38], and the effect of microwave heating temperature in a limited temperature range was also presented[39-41].

In this work, the CaO-PSZ was prepared with microwave heating from CaO-doped zircon at a temperature range between 900 °C to 1300 °C, and a heating duration of 1h. The purpose is to provide more details for the potential application of microwave heating on the

preparation of CaO-doped zircon, and systematically studied the optimisation of the stability of CaO-PSZ. The samples were analysed by X-ray diffraction (XRD), Raman spectroscopy (Raman), Fourier transform infrared spectroscopy (FT-IR) and Scanning electron microscopy (SEM), respectively. At the same time, the multiphase transformation of ZrO_2 during microwave heating, the influences of heating temperature on the microwave structure and interfacial properties of PSZ ceramics were focused on enriching the fundamental knowledge of microwave heating and the preparation of PSZ.

2 Materials and Methods

2.1 Materials

In this paper, CaO-doped zircon smelted in an electric arc furnace was received from Zhengzhou, Henan Province, China. The zirconia was then placed in a microwave high-temperature reactor and calcined to obtain partially stabilised zirconia. The element content of partially stabilised zirconia was analysed by the method recommended by the National Standard of the People's Republic of China (GB/T). The results of chemical composition analysis are shown in Table 1, which shows that the contents of main components ZrO_2 was 94.85%, followed by CaO content was 4.0%, and there were small amounts of other components such as Al_2O_3, SiO_2, Fe_2O_3, and TiO_2.

Fig. 1 shows the XRD pattern of the sample. After comparing and analyzing the data of the diffraction peak of the fused zirconia stabilised by calcium oxide with the standard JCPDS card of monoclinic zirconia (Card No.: 37-1484), the standard JCPDS card of tetragonal zirconia (Card No.: 42-1164) and the standard JCPDS card of Cubic Zirconia (Card No.: 49-1642), it can be concluded that: the main phases of the samples were monoclinic zirconia (m-

ZrO_2) and cubic zirconia (c-ZrO_2). Because the differences between the main diffraction peaks of the t-ZrO_2 phase and the c-ZrO_2 phase are indistinguishable in XRD results, the existence of tetragonal zirconia can hardly be confirmed. Besides, the diffraction peak of the stabiliser CaO is absent in the XRD pattern, indicating that the added stabiliser CaO has completely dissolved in the zirconia crystal.

2.2 Material procedure

The heating experiment of fused zirconia was carried out by microwave method, firstly, 50g of fused zirconia stabilised by calcium oxide was weighed with an electronic balance (AL-104) and was subsequently put into a drying oven (FX101-1) to dry at 105 °C for 12 h, and then the dried sample was put into a high-temperature microwave horizontal reactor. The main components of microwave heating furnace are weight guarantee system, material heating system, sample placing tank, programmed temperature control system, cooling water circulation system, computer control system, exhaust device, crucible and infrared temperature detector. The output power of microwave heating was 3kW, and temperately adjusted to calcine the sample at a heating temperature of 900 °C, 1000 °C, 1100 °C, 1200 °C and 1300 °C, respectively. After a heating holding time of 60 min, the samples were cooled till room temperature in the microwave reaction box, and subsequently taken out for characterisation analysis.

2.3. Characterisation

The raw materials were compared with CaO-PSZ products after microwave heating, and characterised by XRD, SEM, Raman and FT-IR, respectively. The influences of temperature on product structure, crystal phase structure and surface micro-morphology under microwave conditions were discussed. In this experiment, the German Bruker D8 Advance A25x model

X-ray diffractometer was used to analyse the phase of the sample. Under the condition of 40kv tube pressure and 20 mA tube flow rate, using Ka ray of the copper target (λ =0.154056nm) as the target source, the zirconia sample was scanned at 5 °C/min, and the zirconia samples were scanned and tested in the range of 10-100 °; The Raman spectrum of Renishaw Raman scope system 1000 in the UK was used to analyse the phase change of the product. The backscattered Raman signal was obtained by a microscope. The holographic notch filter in the spectral scattering detection area was in the range of 100 cm^{-1}-800 cm^{-1}. The samples were analysed by using the American NICOLET-IS10 model Fourier infrared spectrometer, and the surface functional groups of fused zirconia were scanned and analysed in the spectral range of 4000 cm^{-1}-500 cm^{-1}. The microstructure of the products was analysed by employing the field emission scanning electron microscope of the Netherlands XL30ESEM-TM model.

3 Results and discussion

3.1 XRD characterisation

XRD analysis of CaO-PSZ heated at 900 °C, 1000 °C, 1100 °C, 1200 °C and 1300 °C was carried out with a holding time of 1 h. The mineral composition and crystal structure of the samples were analysed, and the amorphous structure and subsequent transformation were observed. The results are shown in Fig. 2.

Fig. 2 shows that the diffraction peaks of prepared CaO-PSZ have planes of (111), (200) and (220) for cubic crystal at 2θ=30.12 °, 34.96 ° and 50.22 °, and also have planes of ($\bar{1}$11) and (111) for monoclinic crystal at 2θ=28.06 ° and 31.24 °. In the products prepared at a heating temperature of 900 °C, c-ZrO_2 and m-ZrO_2 mainly existed. Compared with the diffraction peaks of the original materials, a few of refinement on the characteristic peaks of

the CaO-PSZ samples treated at 900 °C are noticed accompanied with small impurity peaks. The XRD diffraction peaks of the prepared samples are widened, indicating that CaO-PSZ samples heated at 900 °C have a small part of amorphous crystal structure, and the transformation from m-ZrO_2 phase to t-ZrO_2 phase has not yet started. With the continuous temperature rising process, from 1000 °C to 1100 °C, the intensities of diffraction peaks at 2θ = 30.12 °, 34.96 ° and 50.22 ° increased, and the phases at 2θ = 28.06 ° and 31.24 ° gradually decrease. The peak shapes of stable diffraction peaks become more refined, indicating that the grains developed at this stage, and the content of stable phase structure increased resulting from the transformation of the m-ZrO_2 phase to the t-ZrO_2 phase. With a microwave heating temperature ranged from 1200 °C to 1300 °C, the main phase of the calcined sample was cubic ZrO_2 at 2θ = 30.12 °C. However, compared with the XRD pattern for the prepared sample at 1100 °C, the diffraction peak intensity of (111) crystal plane of cubic phase ZrO_2 (JCPDS Card No. 49-1642) at 2θ = 30.12 ° decrease significantly, and the diffraction peak intensity of (111) at 2θ = 28.06 ° is lower than that at 1100 °C. The monoclinic diffraction peaks of $(\bar{1}11)$ crystal plane and (111) crystal plane at 2θ = 28.06 ° and 2θ = 31.24 ° disappear completely. The results show that the increase of heating temperature promoted the calcium ions moved into the ZrO_2 lattice, and was beneficial for the transformation of the m-ZrO_2 phase to t-ZrO_2 phase [42, 43].

3.2 Determination and calculation of stability rate

The "K value semi-quantitative method" was used to calculate the stability factor of the as-received material and the prepared PSZ. The calculation results are shown in Fig. 3 with Eq. (1):

$$Stability\ factor = \frac{Intensity\ of\ 29.92^\circ}{Intensity\ of\ 28.06^\circ + Intensity\ of\ 31.24^\circ + Intensity\ of\ 29.92^\circ} \times 100\% \quad (1)$$

where the intensity of 29.92 ° represents the peak intensity of cubic zirconia; the intensity of 28.06 ° and intensity of 31.24 ° represent the peak intensities of monoclinic zirconia.

Fig. 3 shows that with the increase of heating temperature from 900 °C, 1000 °C，1100 °C，1200 °C and 1300 °C, the stability rate of the prepared PSZ gradually increases from 88.14% (as-received) to 88.51% (at 900 °C), 95.02% (at 1000 °C), 95.17% (at 1100 °C), 96.31% (at 1200 °C) and reaches the peak value of 97.64% at 1300 °C. The change on stabilities of the products shows that at a low heating temperature, the driving force for the phase transformation of m-ZrO_2 phase to t-ZrO_2 phase was small, only a few of tetragonal phase were formed and subsequently changed to monoclinic phase in the cooling process, resulting to a limited amount of tetragonal phase in the final products with relatively low stability factor; With the temperature increasing, the driving force of the phase transformation increased, and a large number of m-ZrO_2 changed to t-ZrO_2 accompanied with the increase of c-ZrO_2. Therefore, in the high-temperature stage, the peak intensity of the m-ZrO_2 phase decreased, whilst the peak intensity of t-ZrO_2 increased, the stability of zirconia increased consequently.

3.3 Raman spectroscopy characterisation

To observe the influence of heating temperature on the microstructure of CaO stabilised zirconia, the phase structure transformation of CaO stabilised zirconia at different temperatures was studied. The as-received sample and the microwave heating products were analysed and characterised by Raman spectroscopy. The duration constant was controlled at 1 h and the temperature was increasing from 900 °C to 1300 °C. The results are shown in Fig. 4.

To avoid the influence of equipment parameters and conditions on signal intensity,

normalised intensity calculated with Eq. (2) was used to divide the Raman data of raw materials, 900 °C, 1000 °C, 1100 °C, 1200 °C and 1300 °C.

$$Normalized\ intensity = \frac{Intensities\ of\ peak\ splitting}{Intensity\ of\ the\ strongest\ peak} \quad (2)$$

The results are shown in Fig. 4(a), indicating that after calcining at 900 °C for 1 h, the Raman bands identified at frequencies of 403 cm^{-1}, 375 cm^{-1}, 350cm^{-1}, 319 cm^{-1} and 284 cm^{-1}. Among them, monoclinic zirconia caused Raman vibration characteristic peaks at 403 cm^{-1}, 375 $cm^{-1}$and 350 cm^{-1}, and tetragonal zirconia caused Raman vibration characteristic peaks at 319 cm^{-1} and 284 cm^{-1}. Agree with the results presented in the XRD spectrum, the existences of the tetragonal phase and monoclinic phase were noticed in the Raman spectrum of all the samples.

The Gaussian mathematical model was used to fit the trajectories of vibration characteristic peaks related to the tetragonal phase and the monoclinic phase. The purpose is to further understand the phase change in the microwave-assisted heating process. As can be seen from Fig. 4(b) to Fig. 4(g), the fitting curves corresponding to Raman data of raw materials, 900 °C, 1000 °C, 1100 °C, 1200 °C and 1300 °C are presented, respectively. In these figures, peak (1) and peak (2) are related to the tetragonal phase and peak (3), peak (4) and peak (5) are related to the monoclinic phase. The R^2 values for the fitting curves presented in Fig. 4(b) to Fig. 4(g) are all above 0.99. Additionally, the corresponding Full Width at Half Maxima (FWHM) of the peaks of the tetragonal phase, namely peak (1) and peak (2) was calculated. For peak (1) in Fig. 4(b) to Fig. 4(g), the corresponding FWHM are 31.81, 29.57, 28.27, 28.19, 26.95 and 27.77, respectively. For peak (2) in Fig. 4(b) to Fig. 4(g), the corresponding FWHM are 13.01, 15.19, 16.71, 15.88, 16.03 and 18.42, respectively. In the studied temperature range, the FWHM of microwave treated sample is averagely

different from that of the raw material, indicating that microwave heating has a significant effect on the microstructure of the raw material.

The value of Area IntgP, calculated based on the percentage of the peak area of the monoclinic/tetragonal phase to the summarised peak area of the monoclinic phase and tetragonal phase, was used to understand the relative percentage content of monoclinic/tetragonal phase. The Area IntgP for the tetragonal phase in Fig. 4(b) to Fig. 4(g) are 20.50%,19.72%, 23.10%, 22.47%, 21.69% and 23.29%, respectively. The Area IntgP for the monoclinic phase in Fig. 4(b) to Fig. 4(g) are 79.49%, 80.29%, 76.91%, 77.52%, 78.32% and 76.71%, respectively. The Area IntgP value of the tetragonal phase was significantly increased with a microwave heating at 1300 °C compared to that of the raw sample, accompanying with the corresponding decrease on the Area IntgP value of monoclinic phase.

3.4 Infrared spectroscopy characterisation

To study the changes of micro surface functional groups of CaO-PSZ heated samples at different temperatures, the FT-IR spectra of samples heated at 900 °C to 1200 °C for 1 h are described in Fig. 5.

Fig. 5 shows that the characteristic peak at 546.40 cm^{-1} in the infrared spectrum of the original sample was resulting from the stretching vibration of Zr-O bond, the absorption peak at 1013.89 cm^{-1} was caused by the bending vibration of O-H bond, and the characteristic absorption peak at 1384.87 cm^{-1} was caused by the sample adsorbing CO_2 in the air, the absorption peak at 1641.74 cm^{-1} was resulting from the bending vibration of H-O-H on the sample surface, and the characteristic absorption peak at 3446.79 cm^{-1} was resulting from the contraction vibration of O-H bond on the sample surface. After heating at 900 °C for 1 h, FT-IR peaks of 544.15 cm^{-1}, 1013.70 cm^{-1}, 1416.99 cm^{-1}, 1641.67 cm^{-1} and 3448.83 cm^{-1} appear,

respectively. After heating at 1000 °C for 1 h, FT-IR peaks of 476.43 cm^{-1}, 1014.27 cm^{-1}, 1416.85 cm^{-1}, 1642.17 cm^{-1} and 3448.61 cm^{-1} appear, respectively. After heating at 1100 °C for 1 h, FT-IR peaks of 546.87 cm^{-1}, 1014.29 cm^{-1}, 1416.22 cm^{-1}, 1642.46 cm^{-1} and 3447.88 cm^{-1} appear, respectively. After heating at 1100 °C for 1 h, FT-IR peaks of 547.08 cm^{-1}, 1013.10 cm^{-1}, 1416.65 cm^{-1}, 1644.15 cm^{-1} and 3449.08 cm^{-1} appear, respectively.

From 900 °C to 1200 °C, the characteristic peak frequency of the Zr-O bond stretching vibration moves to a higher wavenumber, resulting in a blue shift. The blue shift was attributed to the continuous transformation process from m-ZrO_2 to t-ZrO_2, which increased the content of t-ZrO_2 in heated CaO-PSZ samples. At the same time, the wavenumber change of the first infrared peak decreases slowly at this temperature stage, indicating that the phase transition from m-ZrO_2 to t-ZrO_2 tended to be gentle.

With a temperature increase from 1200 °C to 1300 °C, the first infrared spectrum of the heated sample shows a red shift from 547.08 cm^{-1} to 545.78 cm^{-1}, rending to the increasing tendency for the instability of the Zr-O bond.

3.5 SEM characterisation

The SEM was conducted to analyse the surface micromorphology of the sample at different holding temperatures (900 °C, 1000 °C, 1100 °C, 1200 °C and 1300 °C), the results are shown in Fig. 6.

Fig. 6(a) shows that the surface of the as-received sample was rough and the particle shape was irregular. After heating at 900 °C, few morphological changes of the grains are noticed in the area as shown in Fig. 6(b), where irregular and relatively rough surfaces were found; as noticed in Fig. 6(c), the surface of the particles begins to become smooth after heating at 1000 °C, resulting from the phenomenon of particle growth; in Fig. 6(d) and (e),

corresponding to a heating temperature of 1100 °C and 1200 °C, respectively, the edges of the particles were further improved with fewer pores, indicating a good heating effect; in Fig. 6(f), resulting from a heating temperature of 1300 °C, the surface was pore-free, closely combined, few cracks, and some bulges caused by the grain growth. Additionally, the microstructure of heated CaO-PSZ samples became more uniform, indicating that the addition of CaO stabiliser promoted the fusion of grains in ZrO_2 ceramic materials.

4 Conclusions

In this paper, through the analysis and characterisation of the experimental samples, the phase transformation, microstructure and surface morphology changes of CaO-doped zircon during microwave heating were systematically discussed, the following conclusions are drawn:

(1) The increase in heating temperature was useful for the transformation of monoclinic phase zirconia to tetragonal phase zirconia, and thus increasing the stability rate of partially stabilised zirconia.

(2) From the XRD pattern, the intensity of diffraction peaks increases at $2\theta = 30.12°$, 34.96 ° and 50.22 ° while the phase decreases at $2\theta = 28.06°$ and 31.24 ° under microwave heating with a temperature rising from 1000 °C to 1100 °C. The peak shape of the stable diffraction peak becomes finer, indicating that the grains develop at this stage, and the content of the stable phase structure increases due to the transformation of the m-ZrO_2 phase to the t-ZrO_2 phase. Compared with the martensite transformation temperature of 1170 °C under traditional heating conditions, the martensite transformation temperature is lower in the heating stage (<1100 °C) under the microwave heating conditions. The experimental results

also indicate that the martensitic transformation temperature of zirconia from m-ZrO_2 to t-ZrO_2 during the heating stage was reduced under the radiation of microwave energy.

Acknowledgements

Financial supports from the National Natural Science Foundation of China (No: 51764052) and Innovative Research Team (in Science and Technology) at the University of Yunnan Province were sincerely acknowledged.

References

1. *L.L. Fehrenbacher, L.A. Jacobson, Metallographic observation of the monoclinic-tetragonal phase transformation in ZrO2, J. Am. Ceram. Soc. 48(3) (2010) 157-161. .*
2. *C. Sax, C.H. Hämmerle, I. Sailer, 10-year clinical outcomes of fixed dental prostheses with zirconia frameworks, J. Int J Comput Dent, 14(3)(2011) 183-202. .*
3. *B. Stawarczyk, A. Emslander, M. Roos, et al, Zirconia ceramics, their contrast ratio and grain size depending on sintering parameters, J. Dent Mater J, 33(5)(2014) 591-598.*
4. *K.Q. Li, Q. Jiang, J. Chen, J.H. Peng, X.P. Li, S. Koppala, M. Omran, G. Chen, The controlled preparation and stability mechanism of partially stabilized zirconia by microwave intensification, Ceram. Int. 46(6) (2020) 7523-7530. .*
5. *C. Rajababu, P. Bhavani, R.N. Ramamanohar, S.R.I.R. Venkata, Effect of phase transformation on optical and dielectric properties of zirconium oxide nano-particles, Phase Transitions. 88 (2015) 929–938.*
6. *M.R. Álvarez, A.R. Landa, L.C. Otero-Diaz, M.J. Torralvo, Structural and textural study on ZrO2-Y2O3powders, J. Eur. Ceram. Soc. 18 (1998) 1201–1210.*
7. *J. Li, J.H. Peng, S.H. Guo, W.W. Qv, G. Chen, W. Li, L.B. Zhang, Martensitic transformation thermodynamic calculation of ZrO2-MgO system, Phase Transitions. 85 (2012) 1022–1029.*
8. *D.L. Porter, A.H. Heuer, Microstructural development in MgO‐partially stabilized zirconia (Mg‐PSZ), J. Am. Ceram. Soc. 62 (2010) 298‐305.*
9. *A. Ghosh, A.K. Suri, B.T Rao, T.R. Ramamohan, Low-temperature sintering and mechanical property evaluation of nanocrystalline 8 mol% yttria fully stabilized zirconia, J. Journal of the American Ceramic Society, 90(2007) 2015-2023.*
10. *E.C. Grzebielucka, A.S.A. Chinelatto, S.M. Tebcherani. A.L. Chinelatto, Synthesis and sintering of Y2O3-doped ZrO2 powders using two Pechini-type gel routes, J. Ceramics International, 36(2010) 1737-1742.*
11. *Y. Matsumoto, K. Hirota, O. Yamaguchi, S. Fujii, M. Tamamaki, Formation and sintering of corundum-rutile composite powders prepared from alkoxides, J. Materials Research Bulletin, 28(1993) 305-312.*
12. *B.T. Lin, M.D. Jean, J.H. Chou, Using response surface methodology for optimizing deposited partially stabilized zirconia in plasma spraying, Appl. Surf. Sci. 253 (2007) 3254-3262. .*
13. *R.C. Garvie, Structure and thermomechanical properties of partially stabilized zirconia in the CaO-ZrO2 system, J. Am. Ceram. Soc. 55 (2010) 152-157. .*
14. K.Q. Li, J.C., J.H. Peng, S. Koppala, M. Omran, *G. Chen, One-step preparation of CaO-doped partially

stabilized zirconia from fused Zirconia, Ceramics International. 46 (5): 6484-6490.

15. *X.R. Zhang, C.Y. Liu, R. Liu, et al. Coordinating microwave dielectric and optical properties of transparent yttrium aluminum garnet ceramics by regulating spark plasma sintering parameters[J]. Mater. Sci. Eng. B. Solid. State. Mater. Adv. Technol. 260 (2020) 114628.*
16. *W.R. Ting, Academic Process, New York, 1968.*
17. *H.J. Kleebe, W. Braue, H. Schmidt, G. Pezzotti, G. Ziegler, Transmission electron microscopy of microstructures in ceramic materials, J. Eur. ceram. soc. 16 (3) (1996) 339-351.*
18. *K.Q. Li, J. Chen, J.H. Peng, R. Ruan, C. Srinivasakannan, G. Chen, Pilot-scale study on enhanced carbothermal reduction of low-grade pyrolusite using microwave heating, Powder. Technol. 360 (2020) 7523-7530.*
19. *G. Chen, K.Q. Li, Q. Jiang, X.P. Li, J.H. Peng, M. Omran, J. Chen, Microstructure and enhanced volume density properties of FeMn78C8.0 alloy prepared via a cleaner microwave sintering approach, J. Clean. Prod. 262 (2020) 121364. .*
20. *K.Q. Li, G. Chen, J. Chen, J.H. Peng, R. Ruan, C. Srinivasakannan, Microwave pyrolysis of walnut shell for reduction process of low-grade pyrolusite, Bioresource. Technol. 291 (2019) 121838.*
21. *R. Benavente, M.D. Salvador, F.L. Penaranda-Foix, E. Pallone, A. Borrell, Mechanical properties and microstructural evolution of alumina-zirconia nanocomposites by microwave sintering, Ceram. Int. 40 (7) (2014) 11291-11297.*
22. *K. Chihwei, Y. Shen, F. Yen, H. Cheng, I. Hung, S. Wen, M. Wang, M. Stack, Phase transformation behaviour of 3mol% yttria partially-stabilised ZrO2 (3Y-PSZ) precursor powder by an isothermal method, Ceram. Int. 40 (2014) 3243-3251.*
23. *Y. Murase, E. Kato, K. Daimon, Stability of ZrO2 phases in ultrafine ZrO2-Al2O3 mixtures, J. Am. Ceram. Soc. 69 (2) (1986) 83-87.*
24. *K.Q. Li, J. Chen, G. Chen, J.H. Peng, Roger Ruand, C. Srinivasakannane, Microwave dielectric properties and thermochemical characteristics of the mixtures of walnut shell and manganese ore, J. Bioresource Technology. 286 (2019) 121381.*
25. *X.L. Liu, J.M. Xue, F.Y. Ren, et al. Enhanced microwave-absorption properties of polymer-derived SiC/SiOC composite ceramics modified by carbon nanowires[J]. Ceram.Int. 46 (13) 20742-20750.*
26. *J.J. Du, L. Gao, Y. Yang, S.H. Guo, J. Chen, Mamdouh Omran, G. Chen， Modeling and kinetics study of microwave heat drying of low grade manganese ore， J. Advanced Powder Technology, 2020.*
27. *C. Monaco, F. Prete, C. Leonelli, et al. Microstructural study of microwave sintered zirconia for dental applications[J]. Ceram. Int. 41(1) (2015) 1255-1261.*
28. *D.K. Yan, H.A. Zhang, J.Y. Yi, et al. Study on preparation and microwave sintering process of ultra-fine Ti-CN matrix cermet[J]. Hot. Working. Technol. 39 (20) (2010) 73-79. .*
29. *A. Halim, I. Sudin, W.F.F.W. Ali, et al. Formation of Yttria Aluminium Garnet by Microwave Sintering[C]. Mater. Sci. Forum. 5946 (2020) 222-227.*
30. *W.Y. Liu, H.N. Kou, X.F. Wang, L. Bi, X.S. Zhao, Improving the performance of the $Ba_{0.5}Sr_{0.5}Co_{0.8}Fe_{0.2}O_{3-\delta}$ cathode for proton-conducting SOFCs by microwave sintering, J. Ceramics International, 45.16 (2019) 20994-20998.*
31. *Y.L. Ai, Y. Liu, Q.Y. Zhang, Y.X. Gong, W. He, J.J. Zhang, Microwave Sintering of Graphene-Nanoplatelet-Reinforced Al_2O_3 -based Composites, J. Journal of the Korean Ceramic Society, 2018, 55.*
32. *K.Q. Li, G. Chen, X.T. Li, J.H. Peng, R. Ruan, M. Omran, J. Chen, High-temperature dielectric properties and pyrolysis reduction characteristics of different biomass-pyrolusite mixtures in microwave field, Bioresource. Technol. 294 (2019) 122217. .*
33. *K.Q. Li, J. Chen, J.H. Peng, M. Omran, G. Chen, Efficient improvement for dissociation behavior and*

thermal decomposition of manganese ore by microwave calcination, J. Clean. Prod. 260 (2020) 121074. .

34. *C. Meunier, F. Zuo, N. Peillon, et al. In situ study on microwave sintering of ZTA ceramic: Effect of ZrO2 content on densification, hardness, and toughness[J]. J. Am. Ceram. Soc. 100 (3) (2017) 929-936.*

35. *A.R. Annamalai, P.R. Teja, D.K. Agrawal, et al. Microwave heating synthesis and thermoelectric property characterization of highly dense Ca3Co4O9 bulk[J]. Ceram.Int. 46 (11) 17951-17956. .*

36. *R. Benavente, M.D. Salvador, F.L. Penaranda-Foix, E. Pallone, A. Borrell. Mechanical properties and microstructural evolution of alumina-zirconia nanocomposites by microwave sintering[J]. Ceram Int. 40 (2014) 11291–11297.*

37. *M.Y. Zhang, L. Gao, J.X. Kang, J. Pu, J.H. Peng, M. Omran, G. Chen, Stability optimisation of CaO-doped partially stabilised zirconia by microwave sintering, Ceramics International. 45(2019) 23278-23282. .*

38. *N. Dandapat, S. Ghosh. Development of non-shrinkable ceramic composites for use in high-power microwave tubes[J]. Int. J. Miner. Metall. Mater. 26 (4) (2019) 516.*

39. *G. Chen, Y.Q. Ling, Q.N. Li, H.W. Zheng, K.Q. Li, Q. Jiang, L. Gao, M. Orman, J.H. Peng, J. Chen, Stability properties and structural characteristics of CaO-partially stabilized zirconia ceramics synthesized from fused ZrO2 by microwave sintering, Ceram. Int. 46(10) (2020) 16842-16848.*

40. *G. Chen, Y.Q. Ling, Q.N. Li, H.W. Zheng, K.Q. Li, Q. Jiang, J. Chen, M. Orman, L. Gao, Crystal structure and thermomechanical properties of CaO-PSZ ceramics synthesised from fused ZrO2, Ceram. Int. 46(10) (2020) 15357-15363. .*

41. *W.R. Wang, H.F. Xie, L. Xie, et al. Anti-penetration performance of high entropy alloy–ceramic gradient composites[J]. Int. J. Miner. Metall. Mater. 25 (11) (2018) 1320.*

42. *A. Bogicevic, C. Wolverton, G.M. Crosbie, E.B. Stechel, Defect ordering in aliovalently doped cubic zirconia from first principles. Phys. Rev. B. 64(1) (2001) 014106. .*

43. *S. Fabris, A.T. Paxton, M.W. Finnis, A stabilization mechanism of zirconia based on oxygen vacancies only. Acta. Mater. 50(20) (2002) 5171-5178.*

Table captions

Table 1 Chemical composition analysis of calcium oxide doped PSZ samples.

Figure captions

Fig. 1. XRD spectral analysis of PSZ samples doped with calcium oxide.

Fig. 2. Patterns of XRD for CaO-PSZ with heating temperature of 900 °C, 1000 °C, 1100 °C, 1200 °C and 1300 °C respectively and holding time of 1h

Fig. 3. The effect of holding temperature on the stability of heated products.

Fig. 4. (a)Raman spectra of the raw material and microwave heating samples;(b)corresponding fitting diagram of the raw material, corresponding fitting diagram of CaO-PSZ heated at (c)900 °C, (d)1000 °C, (e)1100 °C, (f)1200 °C and (g)1300 °C, with a holding time of 1 h.

Fig. 5. Infrared spectrum of CaO-PSZ heated at 900 °C, 1000 °C, 1100 °C, 1200 °C and 1300 °C, holding time of 1h.

Fig. 6. SEM images of samples with different heating temperatures heated by microwave. (a) raw sample; (b) 900 °C; (c) 1000 °C; (d) 1100 °C; (e) 1200 °C; (f) 1300 °C.

Table 1 Chemical composition analysis of calcium oxide doped PSZ samples.

Composition	ZrO_2	CaO	Al_2O_3	SiO_2	Fe_2O_3	TiO_2
Mass/W%	94.85	4.0	0.4	0.4	0.15	0.2

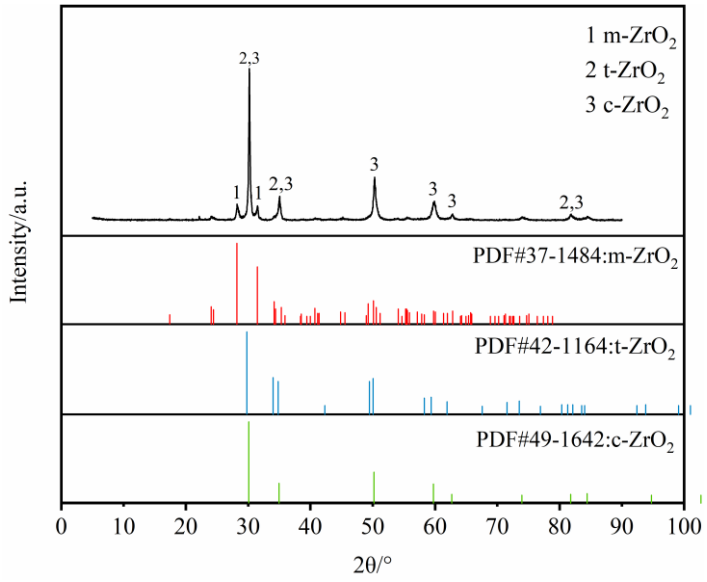

Fig. 1. XRD spectral analysis of PSZ samples doped with calcium oxide.

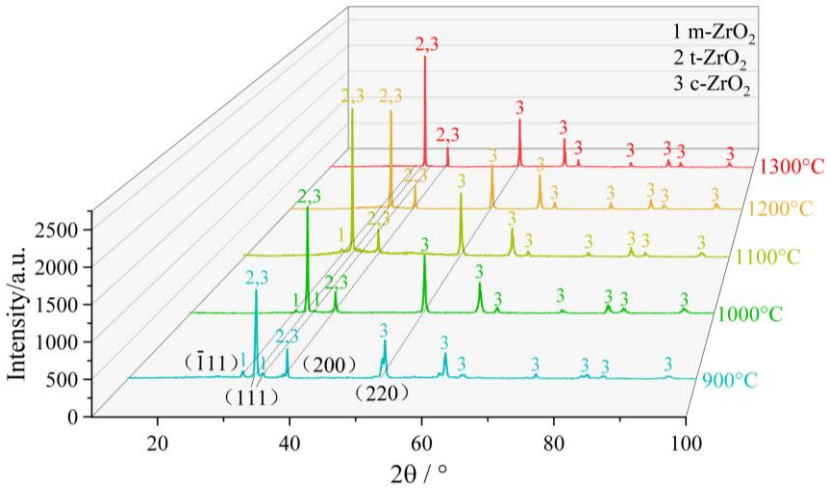

Fig. 2. Patterns of XRD for CaO-PSZ with heating temperature of 900 °C, 1000 °C, 1100 °C, 1200 °C and 1300 °C respectively and holding time of 1h

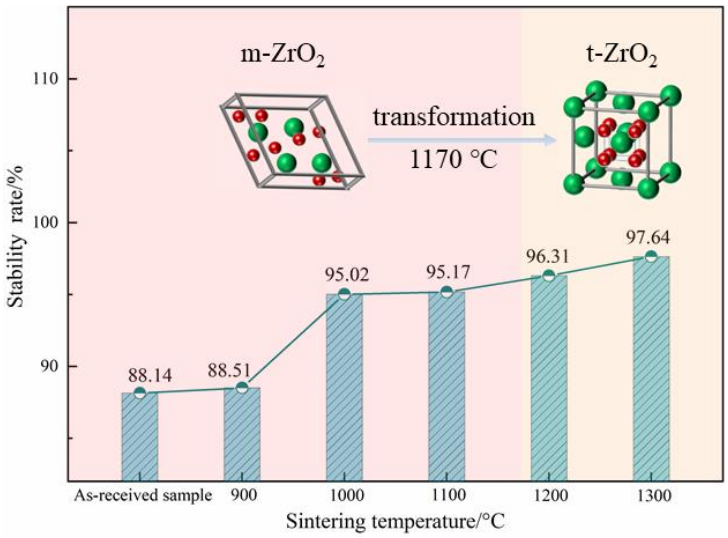

Fig. 3. The effect of holding temperature on the stability of heated products.

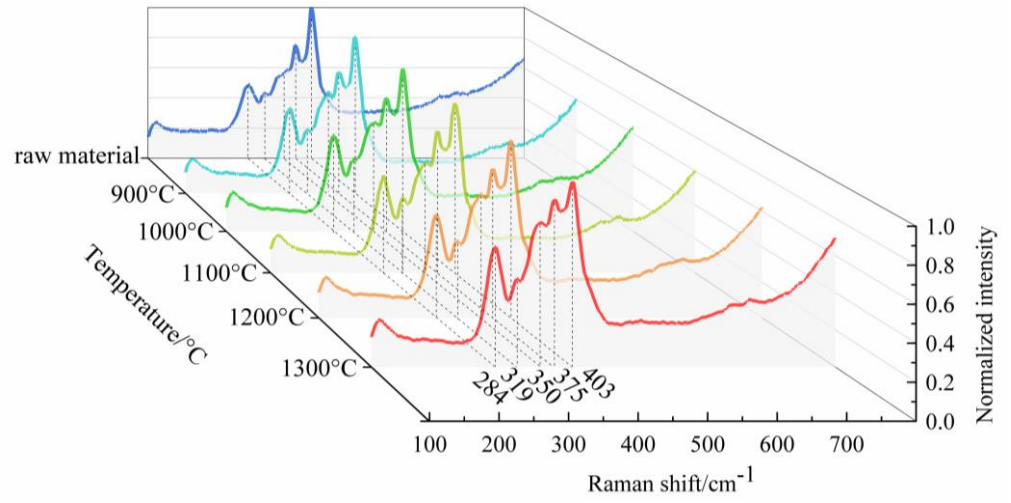

(a)

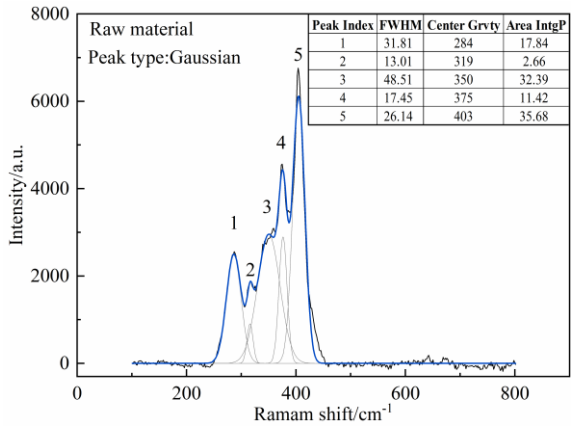

(b)

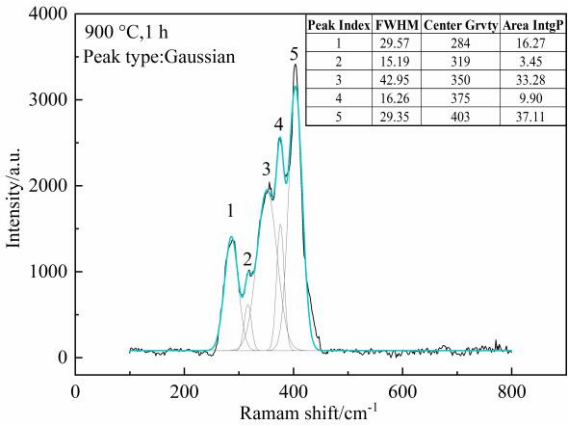

(c)

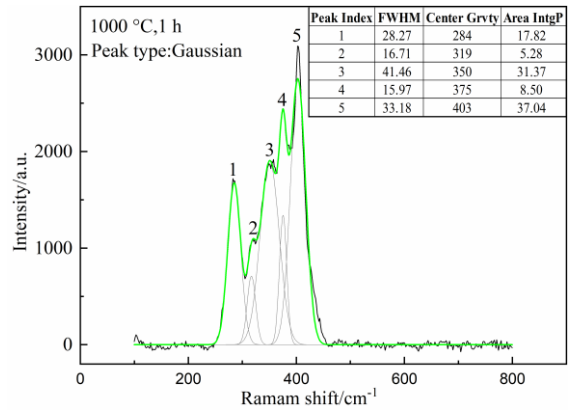

(d)

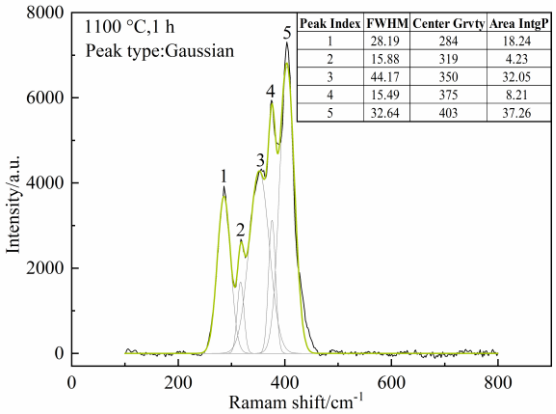

(e)

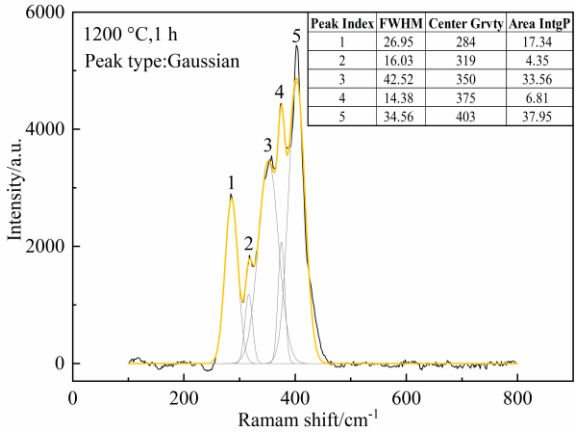

(f)

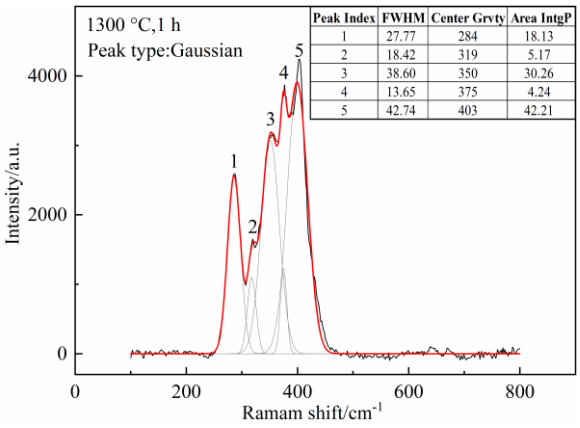

(g)

Fig. 4. (a)Raman spectra of the raw material and microwave heating samples; (b)corresponding fitting diagram of the raw material, corresponding fitting diagram of CaO-PSZ heated at (c)900 °C, (d)1000 °C, (e)1100 °C, (f)1200 °C and (g)1300 °C, with a holding time of 1 h.

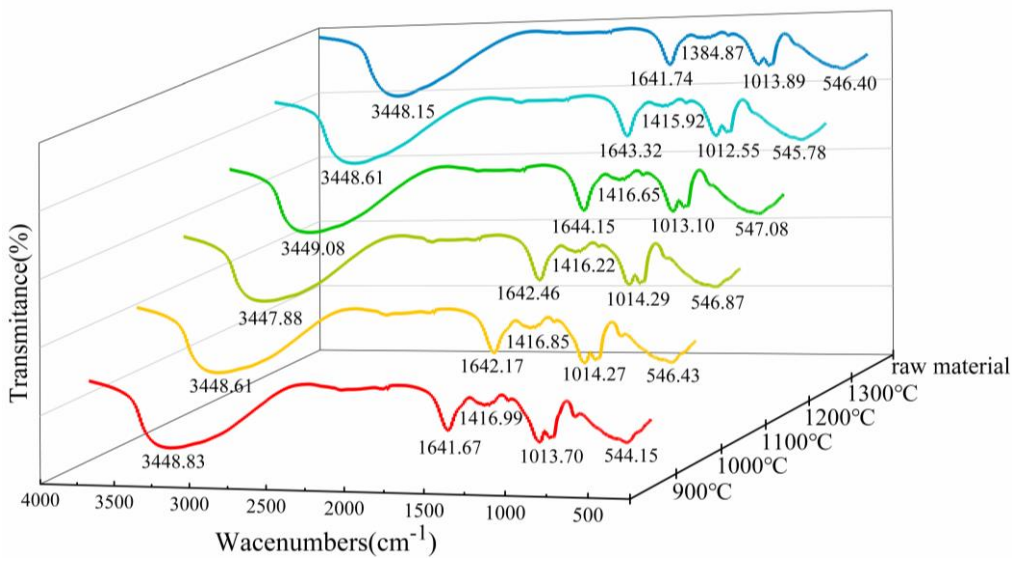

Fig. 5. Infrared spectrum of CaO-PSZ heated at 900 °C, 1000 °C, 1100 °C, 1200 °C and 1300 °C, holding time of 1h.

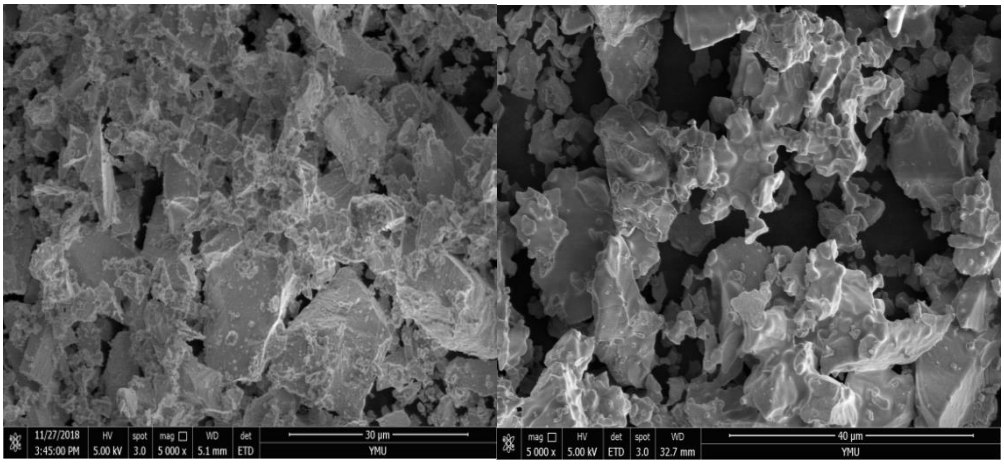

(a) (b)

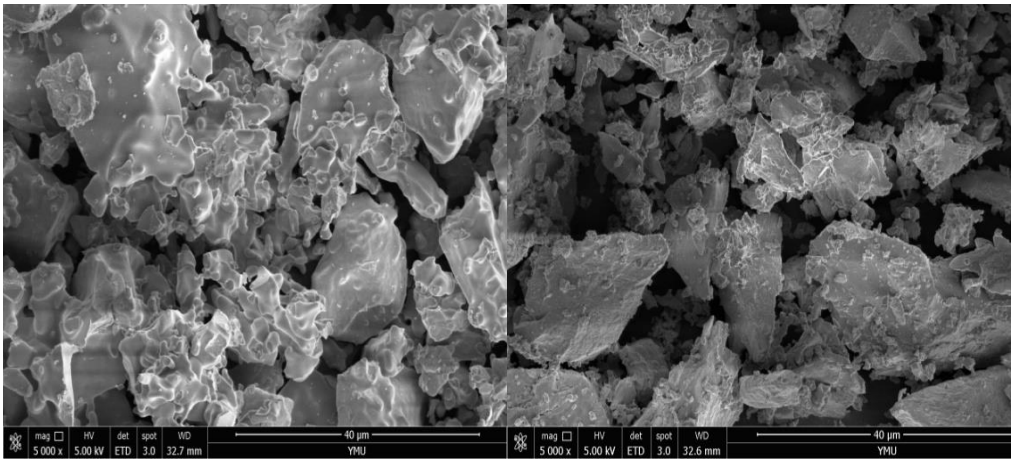

(c) (d)

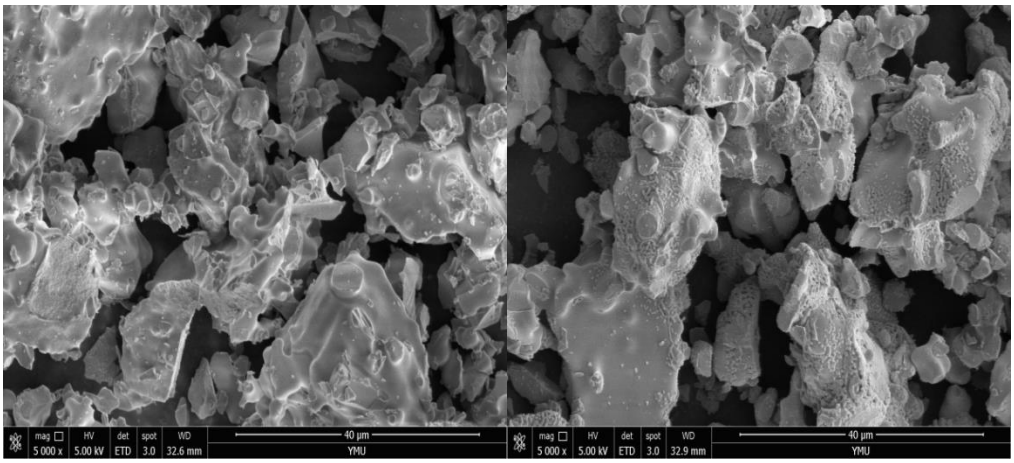

(e) (f)

Fig. 6. SEM images of samples with different heating temperatures heated by microwave. (a) raw sample; (b) 900 °C; (c) 1000 °C; (d) 1100 °C; (e) 1200 °C; (f) 1300 °C.

Optimisation on the stability of CaO-doped partially stabilised zirconia by microwave heating

Yeqing Ling [a, b], Qiannan Li [a, b], Hewen Zheng [a, b], Mamdouh Omran [c], Lei Gao [a, *], Jin Chen [b, **], Guo Chen [a, b, **]

[a] *Kunming Key Laboratory of Energy Materials Chemistry, Key Laboratory of Green-Chemistry Materials in University of Yunnan Province, Yunnan Minzu University, Kunming 650500, PR China.*

[b] *Key Laboratory of Unconventional Metallurgy, Ministry of Education, Kunming University of Science and Technology, Kunming 650500, PR China.*

[c] *Faculty of Technology, University of Oulu, Finland.*

[*] Corresponding author: glkust2013@hotmail.com

[**] Co-corresponding author: jinchen@kust.edu.cn, guochen@kust.edu.cn

Abstract

Partially stabilised zirconia has advantages for the applications in the metallurgical processes which have special requirements in corrosion resistance and high-temperature performance. In the present work, controllable microwave heating was used for the uniform thermal field and consequent microstructure improvement to further improve the stability of partially stabilised zirconia, which was 88.14% prepared by electric arc melting. Analyses including X-ray diffraction (XRD), Scanning electron microscopy (SEM), Fourier transform infrared spectroscopy (FTIR) and Raman spectroscopy (Raman) were used to study the effect of temperature change on the phase composition and structure of the samples. After heating at temperatures of 900 °C, 1000 °C, 1100 °C, 1200 °C and 1300 °C for 1h, the stabilities of the

heated product were 88.51%, 95.02%, 95.17%, 96.31% and 97.64%, respectively. From the phase transformations based on the experimental results, the discussion indicates that the martensitic transformation temperature of zirconia from m-ZrO_2 to t-ZrO_2 during the heating stage was reduced under the radiation of microwave energy.

Keywords: microwave heating

; calcium oxide doped partially stabilised zirconia; stability ratio; phase transition

1 Introduction

Zirconia (ZrO_2) has excellent properties for industrial applications, which have the advantages of high melting point and hardness, low thermal conductivity and thermal expansion coefficient, high refractive index and dielectric parameters, good biocompatibility, difficult corrosion. Therefore, zirconia has become an important inorganic nonmetallic material and has been widely concerned for the applications including refractory, gas turbine, ceramic materials and grinding materials. However, pure zirconia performs unsatisfactory thermal-shock resistance during high-temperature heating or cooling treatment process, resulting from volume-expansion-induced cracking. The cracking occurs because of phase transformation and the subsequent changes in shear stress and volume[1]. For the phase transformation of tetragonal(t-ZrO_2)-to-monoclinic (m-ZrO_2), crackings appear in a normal transformation direction at a temperature below 1000 °C, and also happens in a reverse transformation direction above the temperature of 1173 °C[2-4].

To improve the stability of various properties of ZrO_2, one promising solution is to dope stabilisers to replace Zr^{4+} ion and consequently forming a stable replacement solid solution, which will optimise the internal microstructure of the crystal structure[5]. Various studies have

shown that suitable doping stabilisers including Y_2O_3[6], CaO[7], Al_2O_3, MgO[8] and Sc_2O_3. As a result of doping, the cell volume in zirconia increases, thus the vacancy around zirconium ion reduces the repulsive force between O^{2-}-O^{2-} in the crystal, leading to a distorted coordination layer which effectively inhibits the phase transformation. Consequently, doping prevents the martensitic phase transformation, and thus keeps the tetragonal phase with during the cooling process [9-11]. By controlling the quantity and type of stabilisers, ZrO_2 can be divided into three types of materials from the perspective of microstructure with different stable states doped and crystal size. The mentioned types of ZrO_2 are tetragonal zirconia polycrystalline (TZP), fully stabilised zirconia (FSZ) and partially stabilised zirconia (PSZ) which is a vigorous developed toughening ceramic material contains the tetragonal phase of zirconia[12]. At present, the main preparation method of PSZ ceramic materials is the arc melting method which has high requirements on temperature and disadvantages including long operation time and large energy consumption. The technique also results in low performance on the stability of prepared PSZ materials, which greatly limits the application of this potential ceramic material[13]. It is urgent to develop a low consumption and high-performance preparation method for PSZ ceramic.

Microwave heating technology has great potential as an alternative method for the preparation of PSZ ceramic and has received wide attention[14, 15]. The concept of microwave heating technology was firstly proposed in the mid-1960s[16]. In the middle and late 1980s, microwave heating technology was introduced into the fast preparation of materials and was used as an alternative heating method for the preparation of powder metal[17]. After the 1990s, the technology has developed rapidly in the fields of mineral processing, polymer, nano-organic synthesis and the preparation of special materials. Nowadays, microwave heating

technology has become a key technical method for the efficient preparation of various optimised and modified novel materials based on its advantages[18-20], including selective heating, effective refinement on particle size and microstructure and improved heating uniformity[21-23]. These advantages are resulting from the unique microwave heating mechanism. Microwave can penetrate materials since it is a kind of high-frequency electromagnetic wave(0.3Hz-300GHz). Under the radiation of microwave energy, the material can be fast heated with a uniform thermal field resulting from dielectric loss determined by the microwave absorbing properties including dielectric constant and loss tangent coefficient. A series of studies on the preparation and treatment of ores by the microwave-assisted method were carried out, and FeMn78C8.0 bulk with high density property and low phosphorus was successfully prepared by green microwave heating process[19]; Microwave carbon thermal reduction process for the treatment of manganese ore was used and provided an application reference for microwave reduction of biomass minerals[24, 25]; The microwave drying characteristics of manganese ore were investigated along with the drying mechanism using dynamics and fitting analysis, thus microwave absorption rate in high water content area was promoted [26]. Monaco et al. [27] studied the possibility of low-temperature preparation of ZrO_2 by single-mode and multi-mode microwave heating methods, respectively. At the heating temperature of 1200 °C and the heating cycle of 6 min, the same density can be achieved as that of traditional heating (1450 °C, 600 min). Yan et al. [28] studied the effects of heating temperature and holding time on the mechanical properties of ultrafine Ti (C, N) - based cermets. The results show that the shrinkage, density, bending strength and hardness of ultrafine Ti (C, N) - based cermets increase with the heating temperature increasing to 1500 °C. The results show that the material has fine grains and excellent properties at 1500 °C

for 30 min. Ahmad et al. [29] prepared polycrystalline yttrium aluminium garnet (YAG) ceramic by microwave heating. Micron-sized of Al_2O_3 and Y_2O_3 powders were mixed through in house fabrication mixer for 24 hours before calcined at 1100 °C and palletization process. While both grain sizes and density of heated samples were found increased from 1.4 μm to 2.46 μm and 90% to 98%, respectively. Therefore, microwave heating has a significant effect on the densification behaviour of YAG.

Under the action of the microwave electromagnetic field, ceramic materials will produce a series of dielectric polarization, such as electronic polarization, atomic polarization, dipole turn polarization and interface polarization. In the previous study, $Ba_{0.5}Sr_{0.5}Co_{0.8}Fe_{0.2}O_{3-\delta}$ (BSCF) cathode layer for fuel cells was prepared by a method based on microwave heating[30]. Different from the traditional preparation method for BSCF with a heating temperature of 1000 °C for several hours, the cathode layer can be well bonded with BSCF after heating at 900 °C for 10 minutes under microwave condition. The BSCF layer maintains the microstructure required for the cathodic reaction, effectively reduces the element diffusion between the cathode layer and $BaZr_{0.1}Ce_{0.7}Y_{0.2}O_{3-\delta}$ electrolyte and improves the resistance value. Besides, the power output of BSCF-battery in the microwave group is 0.96 W/cm^2 at 700 °C, which is higher than that of conventional cathode-battery (0.33 W/cm^2). Al_2O_3 ceramics and Al_2O_3 matrix composites with different graphene nanoplatelets (GPL) content were prepared by microwave heating at 1500 °C[31]. The dispersion of GPL in N-methyl pyrrolidone was optimised to depolymerise GPL without destroying its structure. With the addition of GPLs, the microstructure of the composites was further refined and the compactness of the composites was improved. With an optimised value of GPLs% equals to 0.4%, the hardness, fracture toughness and bending strength of the prepared specimen are in

the best state. The research shows that compared with that prepared by conventional heating, ceramic materials prepared by microwave heating have higher density and hardness, more uniform microstructure and better toughness, and the technology was also noticed with high operation efficiency and low energy consumption[32, 33]. Christophe et al. [34] investigated a better understanding of the effect of multimode-microwave heating of zirconia-toughened alumina (ZTA). A comparative dilatometric analysis was conducted between conventional and microwave heating processes, to clarify the influence of zirconia on the densification of ZTA under electromagnetic field. Microwave heating creates a finer homogeneous microstructure, with resulting hardness and toughening comparable to those obtained for conventional heating[35]. Compared with conventional methods, the microwave hybrid heating on ZTA reaches almost full density in a shorter time cycle and at a lower heating temperature. Furthermore, microwave heating is a good way to suppress the grain growth of ZTA and to provide a more uniform microstructure. Furthermore, Benavente et al. [36] have shown that ZTA composites heated by microwave have higher density, hardness and young's modulus in comparison to conventional heating. Therefore, replacing conventional heating with microwave heating could effectively enhance the product yield of PSZ ceramic with the advantages including strong penetration, non-ionization and green energy-saving. In our previous study, the influence of microwave heating time on the stability performance was introduced[37, 38], and the effect of microwave heating temperature in a limited temperature range was also presented[39-41].

In this work, the CaO-PSZ was prepared with microwave heating from CaO-doped zircon at a temperature range between 900 °C to 1300 °C, and a heating duration of 1h. The purpose is to provide more details for the potential application of microwave heating on the

preparation of CaO-doped zircon, and systematically studied the optimisation of the stability of CaO-PSZ. The samples were analysed by X-ray diffraction (XRD), Raman spectroscopy (Raman), Fourier transform infrared spectroscopy (FT-IR) and Scanning electron microscopy (SEM), respectively. At the same time, the multiphase transformation of ZrO_2 during microwave heating, the influences of heating temperature on the microwave structure and interfacial properties of PSZ ceramics were focused on enriching the fundamental knowledge of microwave heating and the preparation of PSZ.

2 Materials and Methods

2.1 Materials

In this paper, CaO-doped zircon smelted in an electric arc furnace was received from Zhengzhou, Henan Province, China. The zirconia was then placed in a microwave high-temperature reactor and calcined to obtain partially stabilised zirconia. The element content of partially stabilised zirconia was analysed by the method recommended by the National Standard of the People's Republic of China (GB/T). The results of chemical composition analysis are shown in Table 1, which shows that the contents of main components ZrO_2 was 94.85%, followed by CaO content was 4.0%, and there were small amounts of other components such as Al_2O_3, SiO_2, Fe_2O_3, and TiO_2.

Fig. 1 shows the XRD pattern of the sample. After comparing and analyzing the data of the diffraction peak of the fused zirconia stabilised by calcium oxide with the standard JCPDS card of monoclinic zirconia (Card No.: 37-1484), the standard JCPDS card of tetragonal zirconia (Card No.: 42-1164) and the standard JCPDS card of Cubic Zirconia (Card No.: 49-1642), it can be concluded that: the main phases of the samples were monoclinic zirconia (m-

ZrO_2) and cubic zirconia (c-ZrO_2). Because the differences between the main diffraction peaks of the t-ZrO_2 phase and the c-ZrO_2 phase are indistinguishable in XRD results, the existence of tetragonal zirconia can hardly be confirmed. Besides, the diffraction peak of the stabiliser CaO is absent in the XRD pattern, indicating that the added stabiliser CaO has completely dissolved in the zirconia crystal.

2.2 Material procedure

The heating experiment of fused zirconia was carried out by microwave method, firstly, 50g of fused zirconia stabilised by calcium oxide was weighed with an electronic balance (AL-104) and was subsequently put into a drying oven (FX101-1) to dry at 105 °C for 12 h, and then the dried sample was put into a high-temperature microwave horizontal reactor. The main components of microwave heating furnace are weight guarantee system, material heating system, sample placing tank, programmed temperature control system, cooling water circulation system, computer control system, exhaust device, crucible and infrared temperature detector. The output power of microwave heating was 3kW, and temperately adjusted to calcine the sample at a heating temperature of 900 °C, 1000 °C, 1100 °C, 1200 °C and 1300 °C, respectively. After a heating holding time of 60 min, the samples were cooled till room temperature in the microwave reaction box, and subsequently taken out for characterisation analysis.

2.3. Characterisation

The raw materials were compared with CaO-PSZ products after microwave heating, and characterised by XRD, SEM, Raman and FT-IR, respectively. The influences of temperature on product structure, crystal phase structure and surface micro-morphology under microwave conditions were discussed. In this experiment, the German Bruker D8 Advance A25x model

X-ray diffractometer was used to analyse the phase of the sample. Under the condition of 40kv tube pressure and 20 mA tube flow rate, using Ka ray of the copper target (λ =0.154056nm) as the target source, the zirconia sample was scanned at 5 °C/min, and the zirconia samples were scanned and tested in the range of 10-100 °; The Raman spectrum of Renishaw Raman scope system 1000 in the UK was used to analyse the phase change of the product. The backscattered Raman signal was obtained by a microscope. The holographic notch filter in the spectral scattering detection area was in the range of 100 cm^{-1}-800 cm^{-1}. The samples were analysed by using the American NICOLET-IS10 model Fourier infrared spectrometer, and the surface functional groups of fused zirconia were scanned and analysed in the spectral range of 4000 cm^{-1}-500 cm^{-1}. The microstructure of the products was analysed by employing the field emission scanning electron microscope of the Netherlands XL30ESEM-TM model.

3 Results and discussion

3.1 XRD characterisation

XRD analysis of CaO-PSZ heated at 900 °C, 1000 °C, 1100 °C, 1200 °C and 1300 °C was carried out with a holding time of 1 h. The mineral composition and crystal structure of the samples were analysed, and the amorphous structure and subsequent transformation were observed. The results are shown in Fig. 2.

Fig. 2 shows that the diffraction peaks of prepared CaO-PSZ have planes of (111), (200) and (220) for cubic crystal at 2θ=30.12 °, 34.96 ° and 50.22 °, and also have planes of ($\bar{1}$11) and (111) for monoclinic crystal at 2θ=28.06 ° and 31.24 °. In the products prepared at a heating temperature of 900 °C, c-ZrO_2 and m-ZrO_2 mainly existed. Compared with the diffraction peaks of the original materials, a few of refinement on the characteristic peaks of

the CaO-PSZ samples treated at 900 °C are noticed accompanied with small impurity peaks. The XRD diffraction peaks of the prepared samples are widened, indicating that CaO-PSZ samples heated at 900 °C have a small part of amorphous crystal structure, and the transformation from m-ZrO_2 phase to t-ZrO_2 phase has not yet started. With the continuous temperature rising process, from 1000 °C to 1100 °C, the intensities of diffraction peaks at 2θ = 30.12 °, 34.96 ° and 50.22 ° increased, and the phases at 2θ = 28.06 ° and 31.24 ° gradually decrease. The peak shapes of stable diffraction peaks become more refined, indicating that the grains developed at this stage, and the content of stable phase structure increased resulting from the transformation of the m-ZrO_2 phase to the t-ZrO_2 phase. With a microwave heating temperature ranged from 1200 °C to 1300 °C, the main phase of the calcined sample was cubic ZrO_2 at 2θ = 30.12 °C. However, compared with the XRD pattern for the prepared sample at 1100 °C, the diffraction peak intensity of (111) crystal plane of cubic phase ZrO_2 (JCPDS Card No. 49-1642) at 2θ = 30.12 ° decrease significantly, and the diffraction peak intensity of (111) at 2θ = 28.06 ° is lower than that at 1100 °C. The monoclinic diffraction peaks of $(\bar{1}11)$ crystal plane and (111) crystal plane at 2θ = 28.06 ° and 2θ = 31.24 ° disappear completely. The results show that the increase of heating temperature promoted the calcium ions moved into the ZrO_2 lattice, and was beneficial for the transformation of the m-ZrO_2 phase to t-ZrO_2 phase [42, 43].

3.2 Determination and calculation of stability rate

The "K value semi-quantitative method" was used to calculate the stability factor of the as-received material and the prepared PSZ. The calculation results are shown in Fig. 3 with Eq. (1):

$$Stability\ factor = \frac{Intensity\ of\ 29.92^\circ}{Intensity\ of\ 28.06^\circ + Intensity\ of\ 31.24^\circ + Intensity\ of\ 29.92^\circ} \times 100\% \quad (1)$$

where the intensity of 29.92 ° represents the peak intensity of cubic zirconia; the intensity of 28.06 ° and intensity of 31.24 ° represent the peak intensities of monoclinic zirconia.

Fig. 3 shows that with the increase of heating temperature from 900 °C, 1000 °C，1100 °C，1200 °C and 1300 °C, the stability rate of the prepared PSZ gradually increases from 88.14% (as-received) to 88.51% (at 900 °C), 95.02% (at 1000 °C), 95.17% (at 1100 °C), 96.31% (at 1200 °C) and reaches the peak value of 97.64% at 1300 °C. The change on stabilities of the products shows that at a low heating temperature, the driving force for the phase transformation of m-ZrO_2 phase to t-ZrO_2 phase was small, only a few of tetragonal phase were formed and subsequently changed to monoclinic phase in the cooling process, resulting to a limited amount of tetragonal phase in the final products with relatively low stability factor; With the temperature increasing, the driving force of the phase transformation increased, and a large number of m-ZrO_2 changed to t-ZrO_2 accompanied with the increase of c-ZrO_2. Therefore, in the high-temperature stage, the peak intensity of the m-ZrO_2 phase decreased, whilst the peak intensity of t-ZrO_2 increased, the stability of zirconia increased consequently.

3.3 Raman spectroscopy characterisation

To observe the influence of heating temperature on the microstructure of CaO stabilised zirconia, the phase structure transformation of CaO stabilised zirconia at different temperatures was studied. The as-received sample and the microwave heating products were analysed and characterised by Raman spectroscopy. The duration constant was controlled at 1 h and the temperature was increasing from 900 °C to 1300 °C. The results are shown in Fig. 4.

To avoid the influence of equipment parameters and conditions on signal intensity,

normalised intensity calculated with Eq. (2) was used to divide the Raman data of raw materials, 900 °C, 1000 °C, 1100 °C, 1200 °C and 1300 °C.

$$Normalized\ intensity = \frac{Intensities\ of\ peak\ splitting}{Intensity\ of\ the\ strongest\ peak} \quad (2)$$

The results are shown in Fig. 4(a), indicating that after calcining at 900 °C for 1 h, the Raman bands identified at frequencies of 403 cm^{-1}, 375 cm^{-1}, 350cm^{-1}, 319 cm^{-1} and 284 cm^{-1}. Among them, monoclinic zirconia caused Raman vibration characteristic peaks at 403 cm^{-1}, 375 $cm^{-1}$and 350 cm^{-1}, and tetragonal zirconia caused Raman vibration characteristic peaks at 319 cm^{-1} and 284 cm^{-1}. Agree with the results presented in the XRD spectrum, the existences of the tetragonal phase and monoclinic phase were noticed in the Raman spectrum of all the samples.

The Gaussian mathematical model was used to fit the trajectories of vibration characteristic peaks related to the tetragonal phase and the monoclinic phase. The purpose is to further understand the phase change in the microwave-assisted heating process. As can be seen from Fig. 4(b) to Fig. 4(g), the fitting curves corresponding to Raman data of raw materials, 900 °C, 1000 °C, 1100 °C, 1200 °C and 1300 °C are presented, respectively. In these figures, peak (1) and peak (2) are related to the tetragonal phase and peak (3), peak (4) and peak (5) are related to the monoclinic phase. The R^2 values for the fitting curves presented in Fig. 4(b) to Fig. 4(g) are all above 0.99. Additionally, the corresponding Full Width at Half Maxima (FWHM) of the peaks of the tetragonal phase, namely peak (1) and peak (2) was calculated. For peak (1) in Fig. 4(b) to Fig. 4(g), the corresponding FWHM are 31.81, 29.57, 28.27, 28.19, 26.95 and 27.77, respectively. For peak (2) in Fig. 4(b) to Fig. 4(g), the corresponding FWHM are 13.01, 15.19, 16.71, 15.88, 16.03 and 18.42, respectively. In the studied temperature range, the FWHM of microwave treated sample is averagely

different from that of the raw material, indicating that microwave heating has a significant effect on the microstructure of the raw material.

The value of Area IntgP, calculated based on the percentage of the peak area of the monoclinic/tetragonal phase to the summarised peak area of the monoclinic phase and tetragonal phase, was used to understand the relative percentage content of monoclinic/tetragonal phase. The Area IntgP for the tetragonal phase in Fig. 4(b) to Fig. 4(g) are 20.50%,19.72%, 23.10%, 22.47%, 21.69% and 23.29%, respectively. The Area IntgP for the monoclinic phase in Fig. 4(b) to Fig. 4(g) are 79.49%, 80.29%, 76.91%, 77.52%, 78.32% and 76.71%, respectively. The Area IntgP value of the tetragonal phase was significantly increased with a microwave heating at 1300 °C compared to that of the raw sample, accompanying with the corresponding decrease on the Area IntgP value of monoclinic phase.

3.4 Infrared spectroscopy characterisation

To study the changes of micro surface functional groups of CaO-PSZ heated samples at different temperatures, the FT-IR spectra of samples heated at 900 °C to 1200 °C for 1 h are described in Fig. 5.

Fig. 5 shows that the characteristic peak at 546.40 cm^{-1} in the infrared spectrum of the original sample was resulting from the stretching vibration of Zr-O bond, the absorption peak at 1013.89 cm^{-1} was caused by the bending vibration of O-H bond, and the characteristic absorption peak at 1384.87 cm^{-1} was caused by the sample adsorbing CO_2 in the air, the absorption peak at 1641.74 cm^{-1} was resulting from the bending vibration of H-O-H on the sample surface, and the characteristic absorption peak at 3446.79 cm^{-1} was resulting from the contraction vibration of O-H bond on the sample surface. After heating at 900 °C for 1 h, FT-IR peaks of 544.15 cm^{-1}, 1013.70 cm^{-1}, 1416.99 cm^{-1}, 1641.67 cm^{-1} and 3448.83 cm^{-1} appear,

respectively. After heating at 1000 °C for 1 h, FT-IR peaks of 476.43 cm^{-1}, 1014.27 cm^{-1}, 1416.85 cm^{-1}, 1642.17 cm^{-1} and 3448.61 cm^{-1} appear, respectively. After heating at 1100 °C for 1 h, FT-IR peaks of 546.87 cm^{-1}, 1014.29 cm^{-1}, 1416.22 cm^{-1}, 1642.46 cm^{-1} and 3447.88 cm^{-1} appear, respectively. After heating at 1100 °C for 1 h, FT-IR peaks of 547.08 cm^{-1}, 1013.10 cm^{-1}, 1416.65 cm^{-1}, 1644.15 cm^{-1} and 3449.08 cm^{-1} appear, respectively.

From 900 °C to 1200 °C, the characteristic peak frequency of the Zr-O bond stretching vibration moves to a higher wavenumber, resulting in a blue shift. The blue shift was attributed to the continuous transformation process from m-ZrO_2 to t-ZrO_2, which increased the content of t-ZrO_2 in heated CaO-PSZ samples. At the same time, the wavenumber change of the first infrared peak decreases slowly at this temperature stage, indicating that the phase transition from m-ZrO_2 to t-ZrO_2 tended to be gentle.

With a temperature increase from 1200 °C to 1300 °C, the first infrared spectrum of the heated sample shows a red shift from 547.08 cm^{-1} to 545.78 cm^{-1}, rending to the increasing tendency for the instability of the Zr-O bond.

3.5 SEM characterisation

The SEM was conducted to analyse the surface micromorphology of the sample at different holding temperatures (900 °C, 1000 °C, 1100 °C, 1200 °C and 1300 °C), the results are shown in Fig. 6.

Fig. 6(a) shows that the surface of the as-received sample was rough and the particle shape was irregular. After heating at 900 °C, few morphological changes of the grains are noticed in the area as shown in Fig. 6(b), where irregular and relatively rough surfaces were found; as noticed in Fig. 6(c), the surface of the particles begins to become smooth after heating at 1000 °C, resulting from the phenomenon of particle growth; in Fig. 6(d) and (e),

corresponding to a heating temperature of 1100 °C and 1200 °C, respectively, the edges of the particles were further improved with fewer pores, indicating a good heating effect; in Fig. 6(f), resulting from a heating temperature of 1300 °C, the surface was pore-free, closely combined, few cracks, and some bulges caused by the grain growth. Additionally, the microstructure of heated CaO-PSZ samples became more uniform, indicating that the addition of CaO stabiliser promoted the fusion of grains in ZrO_2 ceramic materials.

4 Conclusions

In this paper, through the analysis and characterisation of the experimental samples, the phase transformation, microstructure and surface morphology changes of CaO-doped zircon during microwave heating were systematically discussed, the following conclusions are drawn:

(1) The increase in heating temperature was useful for the transformation of monoclinic phase zirconia to tetragonal phase zirconia, and thus increasing the stability rate of partially stabilised zirconia.

(2) From the XRD pattern, the intensity of diffraction peaks increases at $2\theta = 30.12°$, 34.96 ° and 50.22 ° while the phase decreases at $2\theta = 28.06°$ and 31.24 ° under microwave heating with a temperature rising from 1000 °C to 1100 °C. The peak shape of the stable diffraction peak becomes finer, indicating that the grains develop at this stage, and the content of the stable phase structure increases due to the transformation of the m-ZrO_2 phase to the t-ZrO_2 phase. Compared with the martensite transformation temperature of 1170 °C under traditional heating conditions, the martensite transformation temperature is lower in the heating stage (<1100 °C) under the microwave heating conditions. The experimental results

also indicate that the martensitic transformation temperature of zirconia from m-ZrO_2 to t-ZrO_2 during the heating stage was reduced under the radiation of microwave energy.

Acknowledgements

Financial supports from the National Natural Science Foundation of China (No: 51764052) and Innovative Research Team (in Science and Technology) at the University of Yunnan Province were sincerely acknowledged.

References

1. *L.L. Fehrenbacher, L.A. Jacobson, Metallographic observation of the monoclinic-tetragonal phase transformation in ZrO2, J. Am. Ceram. Soc. 48(3) (2010) 157-161. .*
2. *C. Sax, C.H. Hämmerle, I. Sailer, 10-year clinical outcomes of fixed dental prostheses with zirconia frameworks, J. Int J Comput Dent, 14(3)(2011) 183-202. .*
3. *B. Stawarczyk, A. Emslander, M. Roos, et al, Zirconia ceramics, their contrast ratio and grain size depending on sintering parameters, J. Dent Mater J, 33(5)(2014) 591-598.*
4. *K.Q. Li, Q. Jiang, J. Chen, J.H. Peng, X.P. Li, S. Koppala, M. Omran, G. Chen, The controlled preparation and stability mechanism of partially stabilized zirconia by microwave intensification, Ceram. Int. 46(6) (2020) 7523-7530. .*
5. *C. Rajababu, P. Bhavani, R.N. Ramamanohar, S.R.I.R. Venkata, Effect of phase transformation on optical and dielectric properties of zirconium oxide nano-particles, Phase Transitions. 88 (2015) 929–938.*
6. *M.R. Álvarez, A.R. Landa, L.C. Otero-Diaz, M.J. Torralvo, Structural and textural study on ZrO2-Y2O3powders, J. Eur. Ceram. Soc. 18 (1998) 1201–1210.*
7. *J. Li, J.H. Peng, S.H. Guo, W.W. Qv, G. Chen, W. Li, L.B. Zhang, Martensitic transformation thermodynamic calculation of ZrO2-MgO system, Phase Transitions. 85 (2012) 1022–1029.*
8. *D.L. Porter, A.H. Heuer, Microstructural development in MgO‐partially stabilized zirconia (Mg‐PSZ), J. Am. Ceram. Soc. 62 (2010) 298‐305.*
9. *A. Ghosh, A.K. Suri, B.T Rao, T.R. Ramamohan, Low-temperature sintering and mechanical property evaluation of nanocrystalline 8 mol% yttria fully stabilized zirconia, J. Journal of the American Ceramic Society, 90(2007) 2015-2023.*
10. *E.C. Grzebielucka, A.S.A. Chinelatto, S.M. Tebcherani. A.L. Chinelatto, Synthesis and sintering of Y2O3-doped ZrO2 powders using two Pechini-type gel routes, J. Ceramics International, 36(2010) 1737-1742.*
11. *Y. Matsumoto, K. Hirota, O. Yamaguchi, S. Fujii, M. Tamamaki, Formation and sintering of corundum-rutile composite powders prepared from alkoxides, J. Materials Research Bulletin, 28(1993) 305-312.*
12. *B.T. Lin, M.D. Jean, J.H. Chou, Using response surface methodology for optimizing deposited partially stabilized zirconia in plasma spraying, Appl. Surf. Sci. 253 (2007) 3254-3262. .*
13. *R.C. Garvie, Structure and thermomechanical properties of partially stabilized zirconia in the CaO-ZrO2 system, J. Am. Ceram. Soc. 55 (2010) 152-157. .*
14. K.Q. Li, J.C., J.H. Peng, S. Koppala, M. Omran, *G. Chen, One-step preparation of CaO-doped partially

stabilized zirconia from fused Zirconia, Ceramics International. 46 (5): 6484-6490.

15. *X.R. Zhang, C.Y. Liu, R. Liu, et al. Coordinating microwave dielectric and optical properties of transparent yttrium aluminum garnet ceramics by regulating spark plasma sintering parameters[J]. Mater. Sci. Eng. B. Solid. State. Mater. Adv. Technol. 260 (2020) 114628.*
16. *W.R. Ting, Academic Process, New York, 1968.*
17. *H.J. Kleebe, W. Braue, H. Schmidt, G. Pezzotti, G. Ziegler, Transmission electron microscopy of microstructures in ceramic materials, J. Eur. ceram. soc. 16 (3) (1996) 339-351.*
18. *K.Q. Li, J. Chen, J.H. Peng, R. Ruan, C. Srinivasakannan, G. Chen, Pilot-scale study on enhanced carbothermal reduction of low-grade pyrolusite using microwave heating, Powder. Technol. 360 (2020) 7523-7530.*
19. *G. Chen, K.Q. Li, Q. Jiang, X.P. Li, J.H. Peng, M. Omran, J. Chen, Microstructure and enhanced volume density properties of FeMn78C8.0 alloy prepared via a cleaner microwave sintering approach, J. Clean. Prod. 262 (2020) 121364. .*
20. *K.Q. Li, G. Chen, J. Chen, J.H. Peng, R. Ruan, C. Srinivasakannan, Microwave pyrolysis of walnut shell for reduction process of low-grade pyrolusite, Bioresource. Technol. 291 (2019) 121838.*
21. *R. Benavente, M.D. Salvador, F.L. Penaranda-Foix, E. Pallone, A. Borrell, Mechanical properties and microstructural evolution of alumina-zirconia nanocomposites by microwave sintering, Ceram. Int. 40 (7) (2014) 11291-11297.*
22. *K. Chihwei, Y. Shen, F. Yen, H. Cheng, I. Hung, S. Wen, M. Wang, M. Stack, Phase transformation behaviour of 3mol% yttria partially-stabilised ZrO2 (3Y-PSZ) precursor powder by an isothermal method, Ceram. Int. 40 (2014) 3243-3251.*
23. *Y. Murase, E. Kato, K. Daimon, Stability of ZrO2 phases in ultrafine ZrO2-Al2O3 mixtures, J. Am. Ceram. Soc. 69 (2) (1986) 83-87.*
24. *K.Q. Li, J. Chen, G. Chen, J.H. Peng, Roger Ruand, C. Srinivasakannane, Microwave dielectric properties and thermochemical characteristics of the mixtures of walnut shell and manganese ore, J. Bioresource Technology. 286 (2019) 121381.*
25. *X.L. Liu, J.M. Xue, F.Y. Ren, et al. Enhanced microwave-absorption properties of polymer-derived SiC/SiOC composite ceramics modified by carbon nanowires[J]. Ceram.Int. 46 (13) 20742-20750.*
26. *J.J. Du, L. Gao, Y. Yang, S.H. Guo, J. Chen, Mamdouh Omran, G. Chen， Modeling and kinetics study of microwave heat drying of low grade manganese ore， J. Advanced Powder Technology, 2020.*
27. *C. Monaco, F. Prete, C. Leonelli, et al. Microstructural study of microwave sintered zirconia for dental applications[J]. Ceram. Int. 41(1) (2015) 1255-1261.*
28. *D.K. Yan, H.A. Zhang, J.Y. Yi, et al. Study on preparation and microwave sintering process of ultra-fine Ti-CN matrix cermet[J]. Hot. Working. Technol. 39 (20) (2010) 73-79. .*
29. *A. Halim, I. Sudin, W.F.F.W. Ali, et al. Formation of Yttria Aluminium Garnet by Microwave Sintering[C]. Mater. Sci. Forum. 5946 (2020) 222-227.*
30. *W.Y. Liu, H.N. Kou, X.F. Wang, L. Bi, X.S. Zhao, Improving the performance of the $Ba_{0.5}Sr_{0.5}Co_{0.8}Fe_{0.2}O_{3-\delta}$ cathode for proton-conducting SOFCs by microwave sintering, J. Ceramics International, 45.16 (2019) 20994-20998.*
31. *Y.L. Ai, Y. Liu, Q.Y. Zhang, Y.X. Gong, W. He, J.J. Zhang, Microwave Sintering of Graphene-Nanoplatelet-Reinforced Al_2O_3 -based Composites, J. Journal of the Korean Ceramic Society, 2018, 55.*
32. *K.Q. Li, G. Chen, X.T. Li, J.H. Peng, R. Ruan, M. Omran, J. Chen, High-temperature dielectric properties and pyrolysis reduction characteristics of different biomass-pyrolusite mixtures in microwave field, Bioresource. Technol. 294 (2019) 122217. .*
33. *K.Q. Li, J. Chen, J.H. Peng, M. Omran, G. Chen, Efficient improvement for dissociation behavior and*

thermal decomposition of manganese ore by microwave calcination, J. Clean. Prod. 260 (2020) 121074. .

34. *C. Meunier, F. Zuo, N. Peillon, et al. In situ study on microwave sintering of ZTA ceramic: Effect of ZrO2 content on densification, hardness, and toughness[J]. J. Am. Ceram. Soc. 100 (3) (2017) 929-936.*
35. *A.R. Annamalai, P.R. Teja, D.K. Agrawal, et al. Microwave heating synthesis and thermoelectric property characterization of highly dense Ca3Co4O9 bulk[J]. Ceram.Int. 46 (11) 17951-17956. .*
36. *R. Benavente, M.D. Salvador, F.L. Penaranda-Foix, E. Pallone, A. Borrell. Mechanical properties and microstructural evolution of alumina-zirconia nanocomposites by microwave sintering[J]. Ceram Int. 40 (2014) 11291–11297.*
37. *M.Y. Zhang, L. Gao, J.X. Kang, J. Pu, J.H. Peng, M. Omran, G. Chen, Stability optimisation of CaO-doped partially stabilised zirconia by microwave sintering, Ceramics International. 45(2019) 23278-23282. .*
38. *N. Dandapat, S. Ghosh. Development of non-shrinkable ceramic composites for use in high-power microwave tubes[J]. Int. J. Miner. Metall. Mater. 26 (4) (2019) 516.*
39. *G. Chen, Y.Q. Ling, Q.N. Li, H.W. Zheng, K.Q. Li, Q. Jiang, L. Gao, M. Orman, J.H. Peng, J. Chen, Stability properties and structural characteristics of CaO-partially stabilized zirconia ceramics synthesized from fused ZrO2 by microwave sintering, Ceram. Int. 46(10) (2020) 16842-16848.*
40. *G. Chen, Y.Q. Ling, Q.N. Li, H.W. Zheng, K.Q. Li, Q. Jiang, J. Chen, M. Orman, L. Gao, Crystal structure and thermomechanical properties of CaO-PSZ ceramics synthesised from fused ZrO2, Ceram. Int. 46(10) (2020) 15357-15363. .*
41. *W.R. Wang, H.F. Xie, L. Xie, et al. Anti-penetration performance of high entropy alloy–ceramic gradient composites[J]. Int. J. Miner. Metall. Mater. 25 (11) (2018) 1320.*
42. *A. Bogicevic, C. Wolverton, G.M. Crosbie, E.B. Stechel, Defect ordering in aliovalently doped cubic zirconia from first principles. Phys. Rev. B. 64(1) (2001) 014106. .*
43. *S. Fabris, A.T. Paxton, M.W. Finnis, A stabilization mechanism of zirconia based on oxygen vacancies only. Acta. Mater. 50(20) (2002) 5171-5178.*

Table captions

Table 1 Chemical composition analysis of calcium oxide doped PSZ samples.

Figure captions

Fig. 1. XRD spectral analysis of PSZ samples doped with calcium oxide.

Fig. 2. Patterns of XRD for CaO-PSZ with heating temperature of 900 °C, 1000 °C, 1100 °C, 1200 °C and 1300 °C respectively and holding time of 1h

Fig. 3. The effect of holding temperature on the stability of heated products.

Fig. 4. (a)Raman spectra of the raw material and microwave heating samples;(b)corresponding fitting diagram of the raw material, corresponding fitting diagram of CaO-PSZ heated at (c)900 °C, (d)1000 °C, (e)1100 °C, (f)1200 °C and (g)1300 °C, with a holding time of 1 h.

Fig. 5. Infrared spectrum of CaO-PSZ heated at 900 °C, 1000 °C, 1100 °C, 1200 °C and 1300 °C, holding time of 1h.

Fig. 6. SEM images of samples with different heating temperatures heated by microwave. (a) raw sample; (b) 900 °C; (c) 1000 °C; (d) 1100 °C; (e) 1200 °C; (f) 1300 °C.

Table 1 Chemical composition analysis of calcium oxide doped PSZ samples.

Composition	ZrO_2	CaO	Al_2O_3	SiO_2	Fe_2O_3	TiO_2
Mass/W%	94.85	4.0	0.4	0.4	0.15	0.2

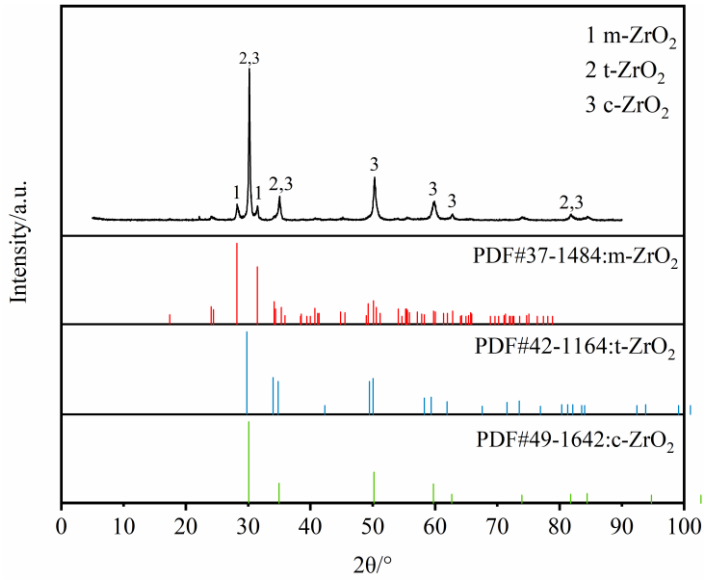

Fig. 1. XRD spectral analysis of PSZ samples doped with calcium oxide.

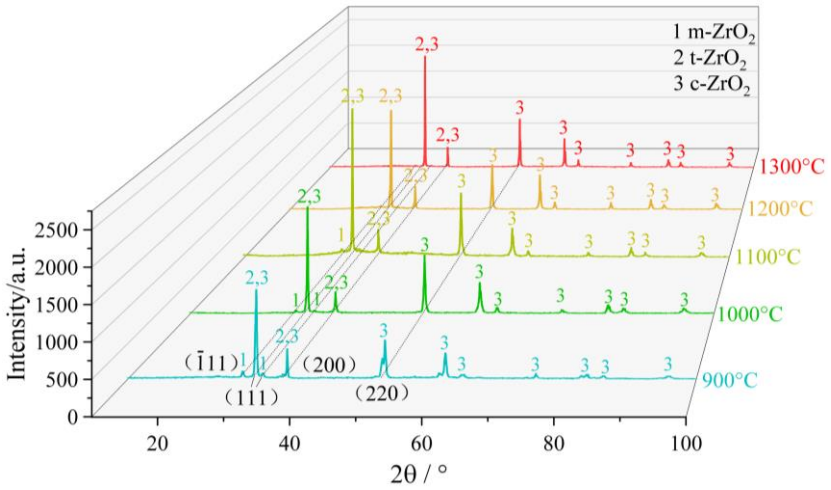

Fig. 2. Patterns of XRD for CaO-PSZ with heating temperature of 900 °C, 1000 °C, 1100 °C, 1200 °C and 1300 °C respectively and holding time of 1h

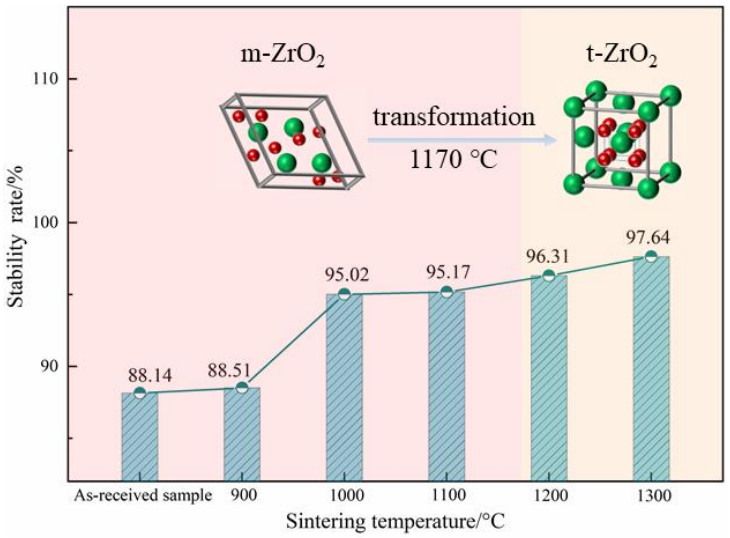

Fig. 3. The effect of holding temperature on the stability of heated products.

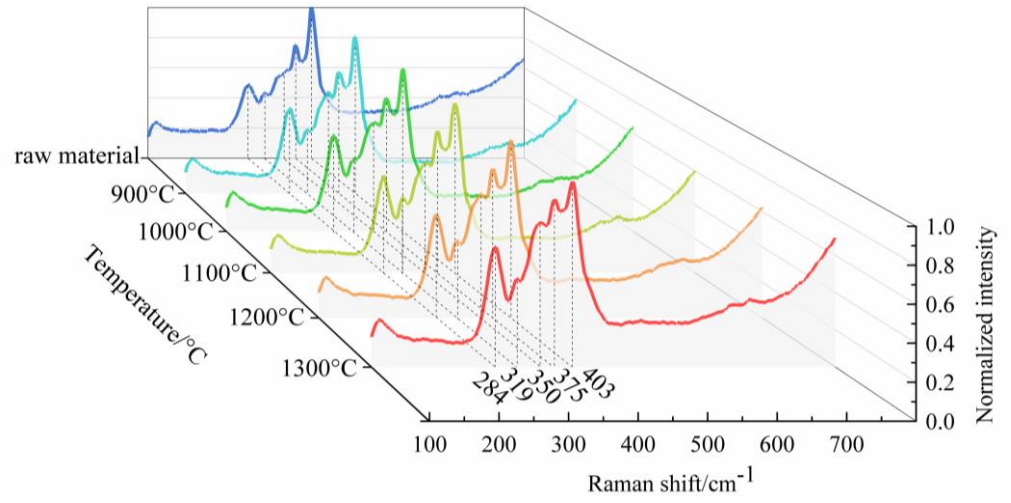

(a)

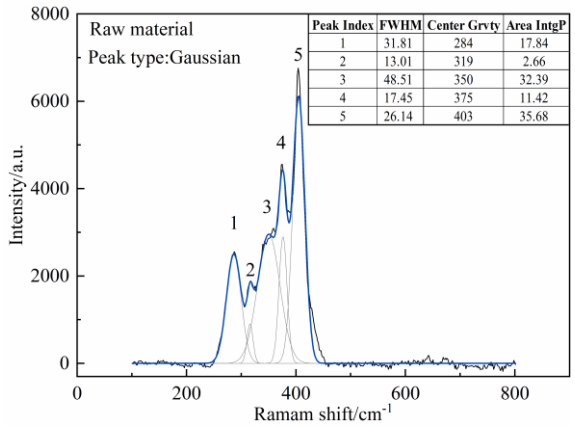

(b)

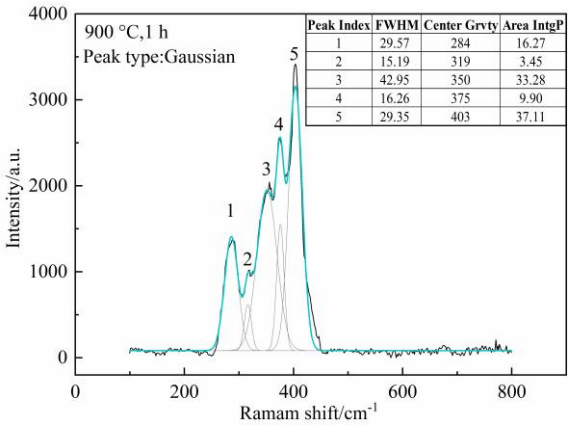

(c)

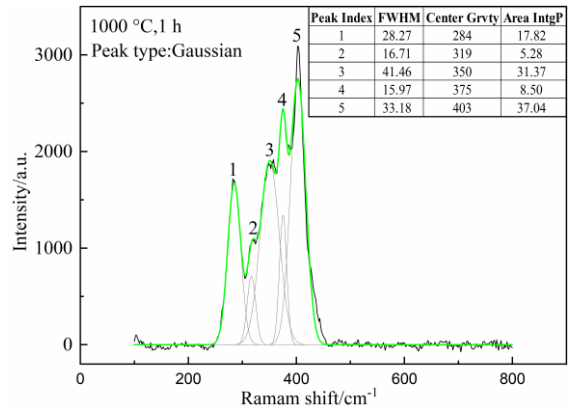

(d)

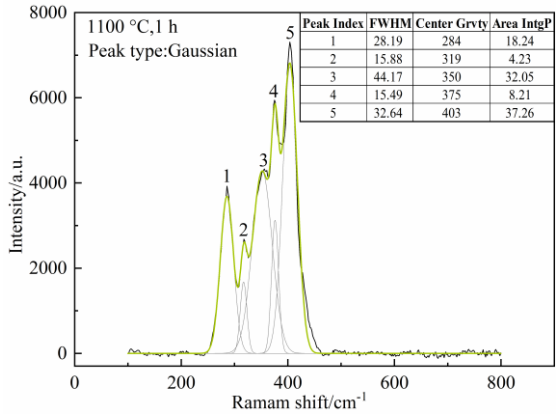

(e)

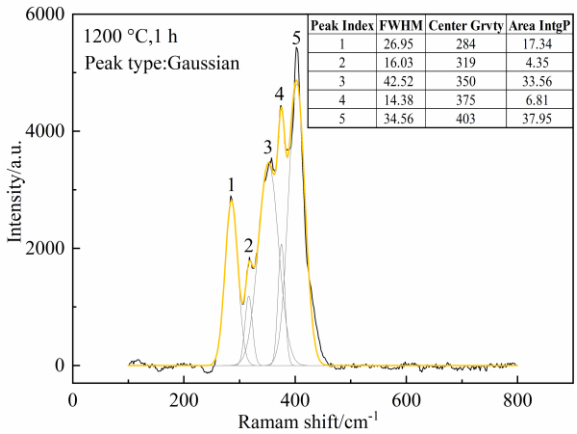

(f)

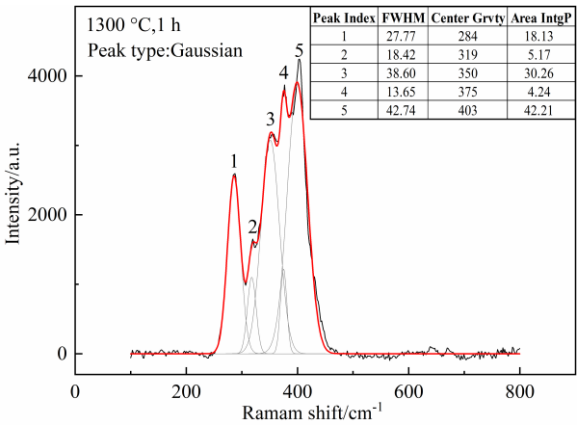

(g)

Fig. 4. (a)Raman spectra of the raw material and microwave heating samples; (b)corresponding fitting diagram of the raw material, corresponding fitting diagram of CaO-PSZ heated at (c)900 °C, (d)1000 °C, (e)1100 °C, (f)1200 °C and (g)1300 °C, with a holding time of 1 h.

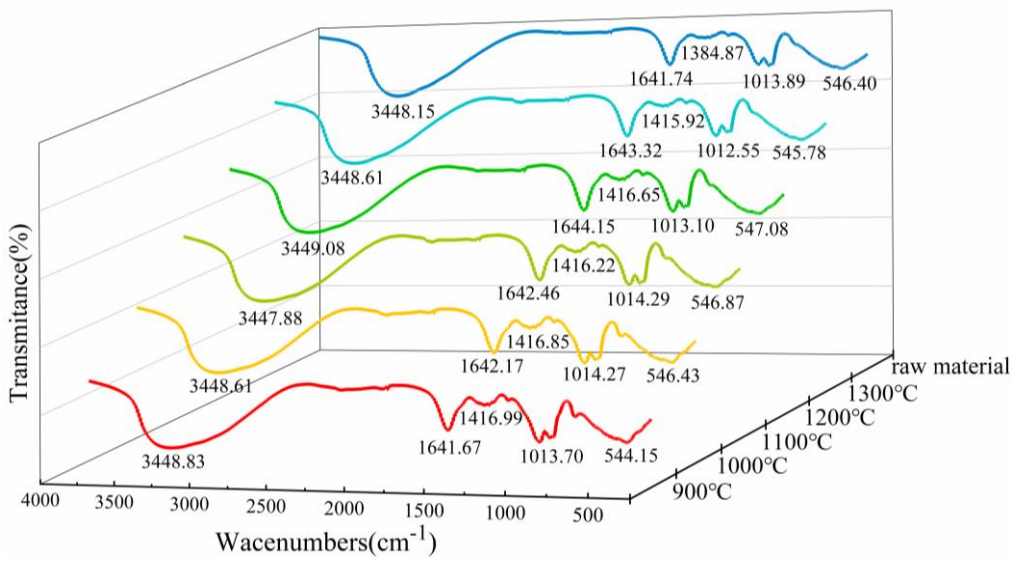

Fig. 5. Infrared spectrum of CaO-PSZ heated at 900 °C, 1000 °C, 1100 °C, 1200 °C and 1300 °C, holding time of 1h.

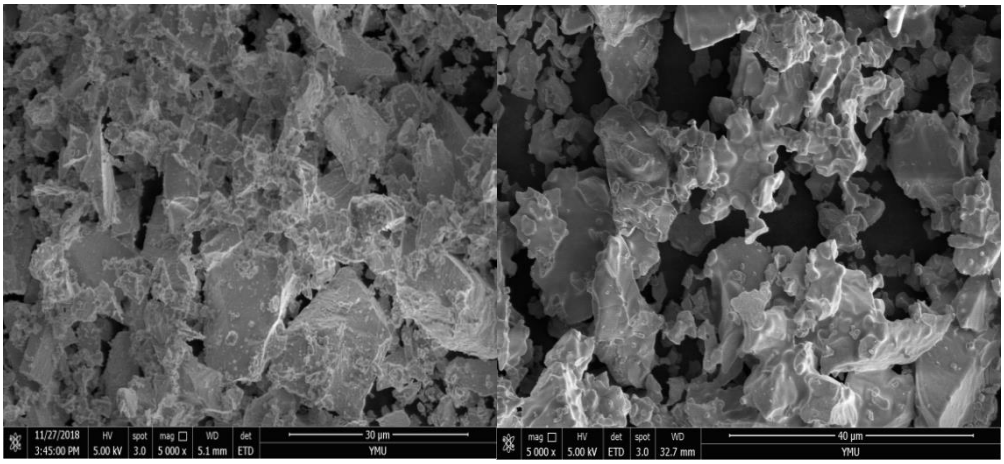

(a) (b)

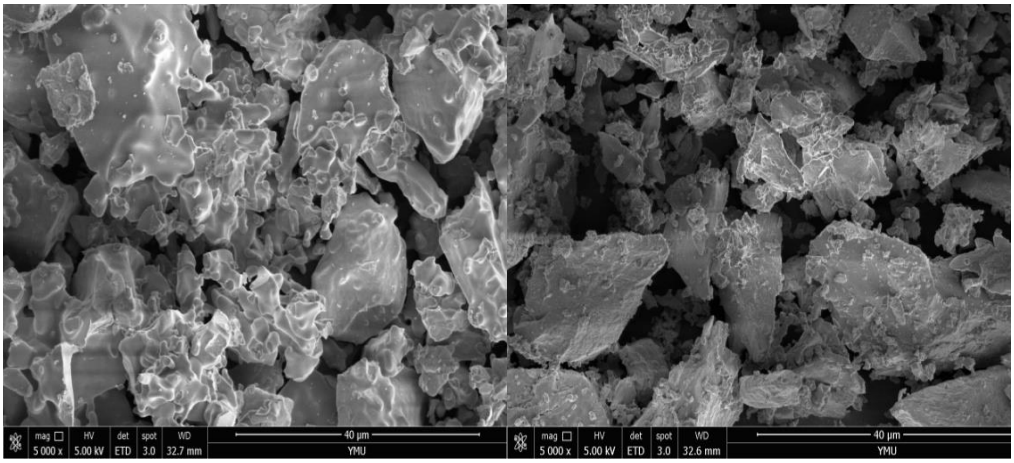

(c) (d)

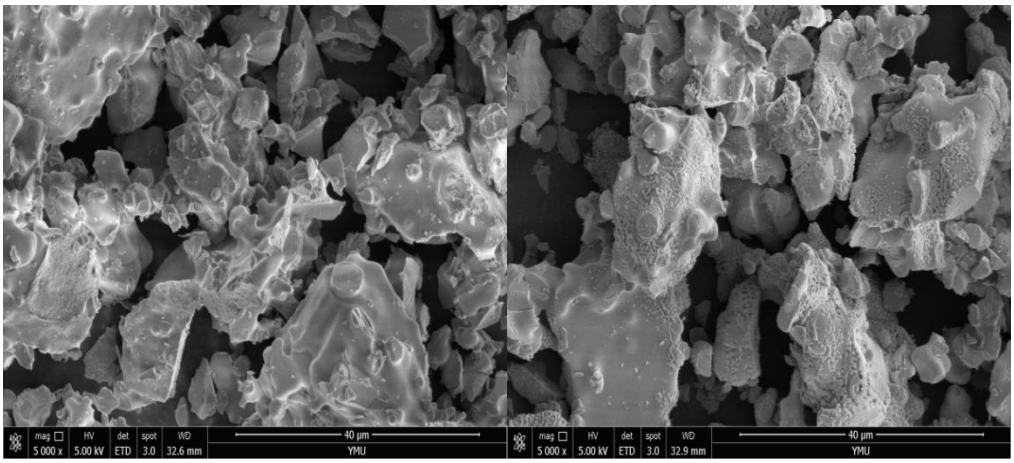

(e) (f)

Fig. 6. SEM images of samples with different heating temperatures heated by microwave. (a) raw sample; (b) 900 °C; (c) 1000 °C; (d) 1100 °C; (e) 1200 °C; (f) 1300 °C.

Conflict of interest statement

We declare that we have no financial and personal relationships with other people or organizations that can inappropriately influence our work, there is no professional or other personal interest of any nature or kind in any product, service and/or company that could be construed as influencing the position presented in, or the review of, the manuscript entitled, "*Optimisation on the stability of CaO-doped partially stabilized zirconia by microwave sintering*" by Yeqing Ling, Qiannan Li, Hewen Zheng, Mamdouh Omran, Lei Gao, Jin Chen and Guo Chen.